



CP -violating observables of four-body $B_{(s)} \rightarrow (\pi\pi)(K\bar{K})$ decays in perturbative QCD

Da-Cheng Yan¹, Yan Yan¹, Zhou Rui^{2,a}

¹ School of Mathematics and Physics, Changzhou University, Changzhou 213164, Jiangsu, China

² College of Sciences, North China University of Science and Technology, Tangshan 063210, Hebei, China

Received: 7 May 2024 / Accepted: 1 July 2024

© The Author(s) 2024

Abstract In this work, we investigate six helicity amplitudes of the four-body $B_{(s)} \rightarrow (\pi\pi)(K\bar{K})$ decays via an angular analysis in the perturbative QCD (PQCD) approach. The $\pi\pi$ invariant mass spectrum is dominated by the vector resonance $\rho(770)$ together with scalar resonance $f_0(980)$, while the vector resonance $\phi(1020)$ and scalar resonance $f_0(980)$ are expected to contribute in the $K\bar{K}$ invariant mass range. We extract the two-body branching ratios $\mathcal{B}(B_{(s)} \rightarrow \rho\phi)$ from the corresponding four-body decays $B_{(s)} \rightarrow \rho\phi \rightarrow (\pi\pi)(K\bar{K})$ based on the narrow width approximation. The predicted $\mathcal{B}(B_s^0 \rightarrow \rho\phi)$ agrees well with the current experimental data within errors. The longitudinal polarization fractions of the $B_{(s)} \rightarrow \rho\phi$ decays are found to be as large as 90%, basically consistent with the previous two-body predictions within uncertainties. In addition to the direct CP asymmetries, the triple-product asymmetries (TPAs) originating from the interference among various helicity amplitudes are also presented for the first time. Since the $B_s^0 \rightarrow \rho^0\phi \rightarrow (\pi^+\pi^-)(K^+K^-)$ decay is induced by both tree and penguin operators, the values of the $\mathcal{A}_{\text{dir}}^{\text{CP}}$ and $\mathcal{A}_{\text{T-true}}^1$ are calculated to be $(21.8_{-3.3}^{+2.7})\%$ and $(-10.23_{-1.56}^{+1.73})\%$ respectively. While for pure penguin decays $B^0 \rightarrow \rho^0\phi \rightarrow (\pi^+\pi^-)(K^+K^-)$ and $B^+ \rightarrow \rho^+\phi \rightarrow (\pi^+\pi^0)(K^+K^-)$, both the direct CP asymmetries and “true” TPAs are naturally expected to be zero in the standard model (SM) due to the absence of the weak phase difference. The “fake” TPAs requiring no weak phase difference are usually none zero for all considered decay channels. The sizable “fake” $\mathcal{A}_{\text{T-fake}}^1 = (-20.92_{-2.80}^{+6.26})\%$ of the $B^0 \rightarrow \rho^0\phi \rightarrow (\pi^+\pi^-)(K^+K^-)$ decay is predicted in the PQCD approach, which provides valuable information on the final-state interactions. The above predictions can be tested by the future LHCb and Belle-II experiments.

1 Introduction

In the past several years, the study of charmless nonleptonic decays of B meson has evoked considerable experimental and theoretical interest, primarily because of the importance of these processes in understanding the phenomenon of CP violation. The decay amplitude for “tree-level” $b \rightarrow u$ transition is much smaller than the one for dominant $b \rightarrow c$ transition due to the ratio of Cabibbo–Kobayashi–Maskawa (CKM) matrix elements $|V_{ub}|^2/|V_{cb}|^2 \approx 10^{-2}$. Transitions to s and d quarks are effective flavor-changing neutral currents proceeding mainly by one-loop “penguin” amplitudes, and are also suppressed. The flavor-changing neutral current decay modes provide a sensitive probe for the effect of physics beyond the SM, since their amplitudes are dominant by the penguin diagrams. The understanding of the relative importance of tree and penguin amplitudes will be crucial in studies of CP asymmetries in B meson decays. A non-vanishing direct CP violation needs the interference of at least two amplitudes with a weak phase difference $\Delta\phi$ and a strong phase difference $\Delta\delta$. The direct CP violation is proportional to $\sin \Delta\phi \sin \Delta\delta$. The key point is that the direct CP violation can only be produced when there is a nonzero strong phase difference. Hence, if the strong phases are quite small, the magnitude of the direct CP violation is close to zero. In this case, there is another class of CP -violating effects which has triggered less attention so far and can reveal the presence of new physics: triple product asymmetries (TPAs). A scalar triple product takes a generic form $\vec{v}_1 \cdot (\vec{v}_2 \times \vec{v}_3)$, where each \vec{v}_i is a spin or momentum of the final-state particle. The TPAs are odd under time reversal (T) and also contribute potential signals of CP violation by the CPT theorem. These TPAs go as $\sin \Delta\phi \cos \Delta\delta$, which provide useful complementary information on direct CP violation. Even in the absence of CP violation effects, T -odd triple products (also called “fake” TPAs), which are proportional

^ae-mail: jindui1127@126.com (corresponding author)

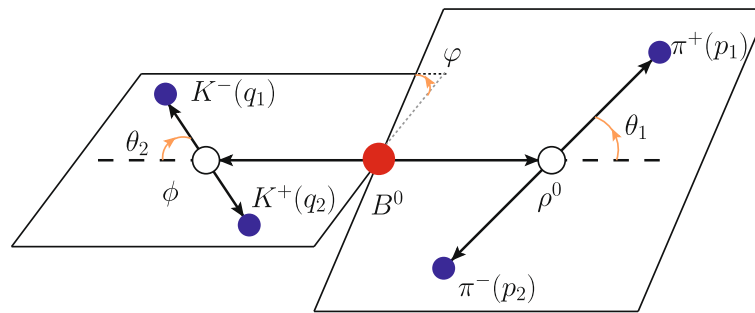


Fig. 1 Graphical definitions of the helicity angles θ_1 , θ_2 and φ for the $B^0 \rightarrow \phi \rho^0$ decay, with each quasi-two-body intermediate resonance decaying to two pseudoscalars ($\rho^0 \rightarrow \pi^+\pi^-$ and $\phi \rightarrow K^+K^-$). $\theta_{1,2}$ is denoted as the angle between the direction of motion of K^- or π^+

in the ϕ or ρ^0 rest frame and ϕ or ρ^0 in the B^0 rest frame, and φ is the angle between the plane defined by K^+K^- and the plane defined by $\pi^+\pi^-$ in the B^0 rest frame

to $\cos \Delta\phi \sin \Delta\delta$, can provide further insight on new physics since most TPAs are expected to be tiny within the SM [1].

A nontrivial triple product requires at least four particles in the final state. $B_{(s)} \rightarrow VV, VS, SV, SS$ decays are usually treated as two-body final states on the theoretical side and have been studied in the two-body framework using various theoretical approaches such as QCD factorization (QCDF) [2–8], PQCD approaches [9–24], the soft-collinear-effective theory (SCET) [25–30] and the factorization-assisted topological amplitude approach (FAT) [31]. While they are at least four-body decays on the experimental side shown in Fig. 1, since the meson $V = \rho, \phi$ is a vector resonance and $S = f_0(980)$ is a scalar resonance with a sizable branching fraction into two pseudoscalar mesons, respectively.¹ The B decays to VV are complicated by the presence of one amplitude with longitudinal polarization A_0 and two amplitudes with transverse polarization A_{\parallel} and A_{\perp} , which is parallel or perpendicular to each other, respectively. The first two states A_0 and A_{\parallel} are CP even, while the last one A_{\perp} is CP odd. Interference between the CP -even (A_0, A_{\parallel}) and CP -odd (A_{\perp}) amplitudes can generate TPAs in angular distributions, which may signal unexpected CP violation due to physics beyond the SM. Recently, TPAs have already been measured by Belle, BABAR, CDF and LHCb Collaborations [32–41]. Phenomenological investigations on TPAs have been conducted intensively in the literature [1, 42–50].

In this work, we study the four-body decays $B_{(s)} \rightarrow (\pi\pi)(K\bar{K})$ in the PQCD approach based on k_T factorization with the relevant Feynman diagrams illustrated in Fig. 2. For a comparison with the LHCb experiment [51], the invariant mass of the $\pi\pi$ pair ranges from 400 to 1600 MeV and the invariant mass for $K\bar{K}$ pair is restricted to be within ± 30 MeV of the known mass of the ϕ meson. The $\pi\pi$ spectrum is dominated by the vector ρ resonance and the scalar resonance f_0 .

¹ For the sake of simplicity, we generally use the abbreviation $f_0 = f_0(980)$, $\rho^0 = \rho(770)^0$, $\phi = \phi(1020)$ in the following sections.

In the considered $K\bar{K}$ invariant-mass range, the vector resonance ϕ is expected to contribute, together with the scalar resonance f_0 . In addition to the branching fractions, the fraction of a given polarization state is an interesting observable and investigated in this work, as well as other observables constructed from the helicity amplitudes like TPAs. As is known, the longitudinal polarization should dominate based on the quark helicity analysis in the factorization assumption [52, 53]. In sharp contrast to these expectations, large transverse polarization (around 50%) is observed in $B \rightarrow K^*\phi$, $B \rightarrow K^*\rho$ and $B_s \rightarrow \phi\phi$ decays [40, 41, 54–56], which poses an interesting challenge for the theory.

It should be stressed that four-body decay is still at its early stage from the theoretical point of view since the factorization formalism that describes a multi-body decay in full phase space is not yet available at present. As a first step, we can only restrict ourselves to the specific kinematical configurations in which each two particles fly colinearly and two pairs of final state particles recoil back in the rest frame of the B meson, see Fig. 1. Then the dynamics associated with the pair of final state mesons can be factorized into a two-meson distribution amplitude (DA) $\Phi_{h_1 h_2}$ [57–63]. Thereby, the typical PQCD factorization formula for the considered four-body decay amplitude can be described,

$$\mathcal{A} = \Phi_B \otimes H \otimes \Phi_{KK} \otimes \Phi_{\pi\pi}, \quad (1)$$

where Φ_B is the universal wave function of the B meson and absorbs the non-perturbative dynamics in the process. The Φ_{KK} ($\Phi_{\pi\pi}$) is the two-hadron DA, which involves the resonant and nonresonant interactions between the two moving collinearly mesons. The hard kernel H describes the dynamics of the strong and electroweak interactions in four-body hadronic decays in a similar way as the one for the corresponding two-body decays. The S and P -wave contributions are parametrized into the corresponding timelike form factors involved in the two-meson DAs, whose normalization form factors are assumed to take the Flatté model [64] for

f_0 , and relativistic Breit–Wigner (BW) function for ϕ [65] and the Gounaris–Sakurai (GS) model [66] for ρ . An important breakthrough in the theory of four-body B meson decays has been achieved based on the quasi-two-body-decay mechanism. Recently, the localized CP violation and branching fraction of the four-body decay $B^0 \rightarrow K^-\pi^+\pi^+\pi^-$ have been calculated by employing a quasi-two-body QCDF approach in Refs. [67,68]. In our previous works [69–73], the PQCD factorization formalism based on the quasi-two-body-decay mechanism for four-body B meson decays has been well established. Within the framework of PQCD approach, the branching ratios and direct CP asymmetries of four-body decays $B_s^0 \rightarrow \pi\pi\pi\pi$ have also been studied [74].

The layout of the present paper is organized as follows. In Sect. 2, we give a brief introduction for the triple product asymmetries analyzed in our work. The kinematics and the formalism of PQCD on four body decays are presented in Sect. 3. The numerical values and some discussions will be given in Sect. 4. Section 5 contains our conclusions. The Appendix A and B collect the S -wave decay amplitudes and the two-meson DAs adopted in our calculations respectively.

2 CP violating observables

2.1 Angular distribution and Helicity amplitudes

Taking the four-body decay $B^0 \rightarrow \rho^0\phi \rightarrow (\pi^+\pi^-)(K^+K^-)$ depicted in Fig. 1 as an example, the study of the angular distribution usually employs three helicity angles: θ_1 , θ_2 and φ . We denote θ_1 (θ_2) as the polar angle between the $\pi^+(K^-)$ direction in the $\pi^+\pi^-(K^+K^-)$ rest frame and the $\pi^+\pi^-(K^+K^-)$ direction in the B^0 rest frame. The angle between the planes defined by $\pi^+\pi^-$ and K^+K^- pairs in the B^0 rest frame will be denoted by φ .

In the four-body decays $B_{(s)} \rightarrow (\pi\pi)(K\bar{K})$, the final state meson pairs $\pi\pi$ and $K\bar{K}$ can be produced in both S and P -wave configurations in the selected invariant mass regions. The total decay amplitudes shall involve six helicity components A_h with $h = VV(3), VS, SV$, and SS , where V and S denote the vector and scalar resonances respectively. The first three, commonly referred to as the P -wave amplitudes, are associated with the final states where both $\pi\pi$ and $K\bar{K}$ pairs come from intermediate vector mesons. Following the definitions given in Refs. [69,70], the P -wave decay amplitudes can be decomposed into three components in the transversity basis, including longitudinal A_0 , parallel A_{\parallel} , and perpendicular A_{\perp} . As the S -wave $\pi\pi$ and $K\bar{K}$ pair can arise from the intermediate resonances R_1 and R_2 labelled in Fig. 2a, the related two single S -wave decay amplitudes are described as A_{SV} and A_{VS} respectively, which are physical different. The double S -wave amplitude A_{SS} is associated with the final states, where both $\pi\pi$ and $K\bar{K}$ meson pairs are generated in

the S wave. All of the above mentioned helicity amplitudes of the four-body decays $B_{(s)} \rightarrow (\pi\pi)(K\bar{K})$ are summarized as follows:

$$\begin{aligned} A_{VV} &: B_{(s)} \rightarrow \rho(\rightarrow \pi\pi)\phi(\rightarrow K\bar{K}), \\ A_{VS} &: B_{(s)} \rightarrow \rho(\rightarrow \pi\pi)f_0(\rightarrow K\bar{K}), \\ A_{SV} &: B_{(s)} \rightarrow f_0(\rightarrow \pi\pi)\phi(\rightarrow K\bar{K}), \\ A_{SS} &: B_{(s)} \rightarrow f_0(\rightarrow \pi\pi)f_0(\rightarrow K\bar{K}). \end{aligned} \tag{2}$$

2.2 Triple-product asymmetries in four-body

$B_{(s)} \rightarrow (\pi\pi)(K\bar{K})$ decays

As stressed in the Introduction, TPAs and direct CP violation can complement each other. TPA is another class of CP -violating effect, which has received considerably less attention and can also reveal the presence of new physics. In this section, we will briefly introduce the TPAs in the present work.

In the four-body decays $B_{(s)} \rightarrow (\pi\pi)(K\bar{K})$, one can usually measure the four final state particles' momenta in the $B_{(s)}$ meson rest frame. We define three unit vectors: \hat{n}_{R_1} (\hat{n}_{R_2}) perpendicular to the R_1 (R_2) decay plane and \hat{z} in the direction of R_1 in the $B_{(s)}$ rest frame. Thus we have

$$\hat{n}_{R_1} \cdot \hat{n}_{R_2} = \cos \varphi, \quad \hat{n}_{R_1} \times \hat{n}_{R_2} = \sin \varphi \hat{z}, \tag{3}$$

implying the T -odd scalar triple products

$$(\hat{n}_{R_1} \times \hat{n}_{R_2}) \cdot \hat{z} = \sin \varphi, \tag{4}$$

$$2(\hat{n}_{R_1} \cdot \hat{n}_{R_2})(\hat{n}_{R_1} \times \hat{n}_{R_2}) \cdot \hat{z} = \sin 2\varphi. \tag{5}$$

A T -odd asymmetry in the B decay can usually be defined by an asymmetry between the number of events with positive and negative values of $\sin \varphi$ or $\sin 2\varphi$,

$$A_T^1 = \frac{\Gamma(\cos \theta_1 \cos \theta_2 \sin \varphi > 0) - \Gamma(\cos \theta_1 \cos \theta_2 \sin \varphi < 0)}{\Gamma(\cos \theta_1 \cos \theta_2 \sin \varphi > 0) + \Gamma(\cos \theta_1 \cos \theta_2 \sin \varphi < 0)}, \tag{6}$$

$$A_T^2 = \frac{\Gamma(\sin 2\varphi > 0) - \Gamma(\sin 2\varphi < 0)}{\Gamma(\sin 2\varphi > 0) + \Gamma(\sin 2\varphi < 0)}. \tag{7}$$

In our calculations, we will focus on the TPAs originating from the interference between the CP -odd amplitude A_{\perp} and the other two CP -even amplitudes A_0 and A_{\parallel} in the $B_{(s)} \rightarrow \rho\phi \rightarrow (\pi\pi)(K\bar{K})$ decays, which can be derived from the partially integrated differential decay rates as [38,45],

$$\begin{aligned} A_T^1 &= \frac{\Gamma(\cos \theta_1 \cos \theta_2 \sin \varphi > 0) - \Gamma(\cos \theta_1 \cos \theta_2 \sin \varphi < 0)}{\Gamma(\cos \theta_1 \cos \theta_2 \sin \varphi > 0) + \Gamma(\cos \theta_1 \cos \theta_2 \sin \varphi < 0)} \\ &= -\frac{2\sqrt{2}}{\pi\mathcal{D}} \int d\omega_1 d\omega_2 k(\omega_1)k(\omega_2)k(\omega_1, \omega_2) \text{Im}[A_{\perp}A_0^*], \end{aligned} \tag{8}$$

$$\begin{aligned} A_T^2 &= \frac{\Gamma(\sin 2\varphi > 0) - \Gamma(\sin 2\varphi < 0)}{\Gamma(\sin 2\varphi > 0) + \Gamma(\sin 2\varphi < 0)} \\ &= -\frac{4}{\pi\mathcal{D}} \int d\omega_1 d\omega_2 k(\omega_1)k(\omega_2)k(\omega_1, \omega_2) \text{Im}[A_{\perp}A_{\parallel}^*], \end{aligned} \tag{9}$$

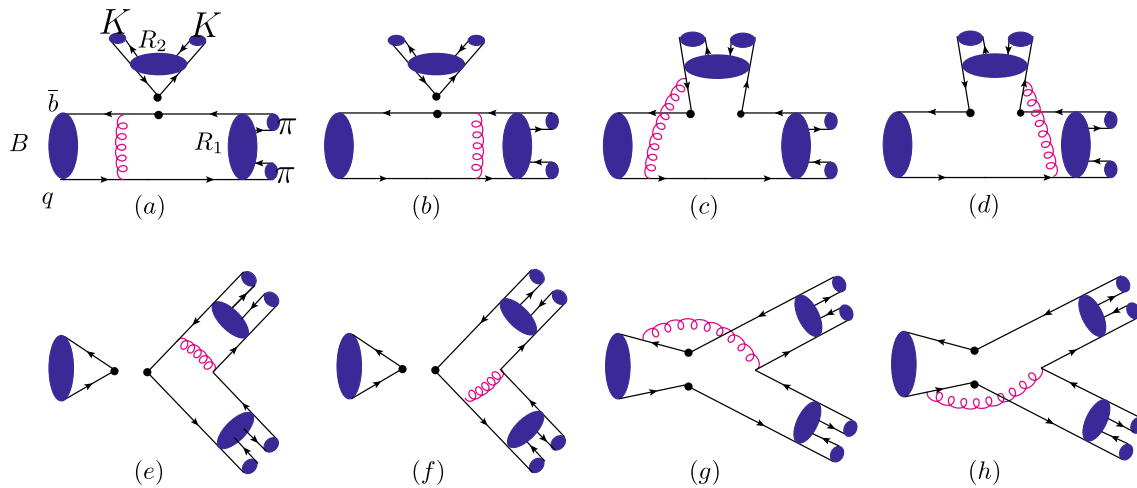


Fig. 2 Typical leading-order Feynman diagrams for the four-body decays $B \rightarrow R_1 R_2 \rightarrow (\pi\pi)(K\bar{K})$ with $q = (d, s)$, where the symbol \bullet denotes a weak interaction vertex. The diagrams (a)–(d) represent the $B \rightarrow (R_1 \rightarrow)\pi\pi$ transition, as well as the diagrams

(e)–(h) for annihilation contributions. If we exchange the position of $R_1 (\rightarrow \pi\pi)$ and $R_2 (\rightarrow K\bar{K})$, we will find the diagrams (a)–(d) for the $B \rightarrow (R_2 \rightarrow)K\bar{K}$ transition

with the denominator

$$\mathcal{D} = \int d\omega_1 d\omega_2 k(\omega_1)k(\omega_2)k(\omega_1, \omega_2) (|A_0|^2 + |A_{\parallel}|^2 + |A_{\perp}|^2), \quad (10)$$

and the invariant mass of the final state meson pair $\omega_{1(2)}$. The factor $k(\omega_1, \omega_2)$ represents the magnitude of the three-momentum of the meson pair in the $B_{(s)}$ meson rest frame,

$$k(\omega_1, \omega_2) = \frac{\sqrt{[m_{B_{(s)}}^2 - (\omega_1 + \omega_2)^2][m_{B_{(s)}}^2 - (\omega_1 - \omega_2)^2]}}{2m_{B_{(s)}}}, \quad (11)$$

where $m_{B_{(s)}}$ is the mass of the $B_{(s)}$ meson. The kinematic variable $k(\omega) = \sqrt{\lambda(\omega^2, m_{h_1}^2, m_{h_2}^2)}/(2\omega)$ is defined in the $h_1 h_2$ center-of-mass frame, with the Källén function $\lambda(a, b, c) = a^2 + b^2 + c^2 - 2(ab + ac + bc)$ and m_{h_1, h_2} being the final state mass.

It should be noted that although the two TPAs given in Eqs. (8) and (9) in terms of transversity amplitudes are odd under time reversal, they are not genuine CP violation. For example, the integrands $\text{Im}(A_{\perp} A_i^*)$ ($i = 0, \parallel$) in the above TPAs can be expanded in the form of $|A_{\perp}| |A_i^*| \sin(\Delta\phi + \Delta\delta)$, with $\Delta\phi$ and $\Delta\delta$ representing the weak and strong phase differences between the two corresponding transversity amplitudes A_{\perp} and A_i^* . The term $|A_{\perp}| |A_i^*| \sin(\Delta\phi + \Delta\delta)$ can be nonzero even in the absence of any weak phases, as long as the strong phase difference $\Delta\delta$ is nonzero. Thus the two TPAs \mathcal{A}_T^1 and \mathcal{A}_T^2 can not reflect a true signal of CP violation. However, one can still obtain a true CP -violating asymmetry by comparing \mathcal{A}_T with $\bar{\mathcal{A}}_T$, where $\bar{\mathcal{A}}_T$ is the T -odd asymmetry

measured in the $\bar{B}_{(s)}$ decay process. We denote the helicity amplitudes for the CP -conjugate decay process by \bar{A}_0 , \bar{A}_{\parallel} and \bar{A}_{\perp} , which can be obtained by applying the following transformations:

$$A_0 \rightarrow \bar{A}_0, \quad A_{\parallel} \rightarrow \bar{A}_{\parallel}, \quad A_{\perp} \rightarrow -\bar{A}_{\perp}. \quad (12)$$

The TPAs of the $\bar{B}_{(s)}$ decays can be defined similarly, but with a multiplicative minus sign. We then have the TPAs for the charge-averaged decay rates

$$\begin{aligned} \mathcal{A}_{T\text{-true}}^{1,\text{ave}} &\equiv \frac{[\Gamma(S_1 > 0) + \bar{\Gamma}(\bar{S}_1 > 0)] - [\Gamma(S_1 < 0) + \bar{\Gamma}(\bar{S}_1 < 0)]}{[\Gamma(S_1 > 0) + \bar{\Gamma}(\bar{S}_1 > 0)] + [\Gamma(S_1 < 0) + \bar{\Gamma}(\bar{S}_1 < 0)]} \\ &= -\frac{2\sqrt{2}}{\pi(\mathcal{D} + \bar{\mathcal{D}})} \int d\omega_1 d\omega_2 k(\omega_1)k(\omega_2)k(\omega_1, \omega_2) \\ &\quad \text{Im}[A_{\perp} A_0^* - \bar{A}_{\perp} \bar{A}_0^*], \end{aligned} \quad (13)$$

$$\begin{aligned} \mathcal{A}_{T\text{-true}}^{2,\text{ave}} &\equiv \frac{[\Gamma(S_2 > 0) + \bar{\Gamma}(\bar{S}_2 > 0)] - [\Gamma(S_2 < 0) + \bar{\Gamma}(\bar{S}_2 < 0)]}{[\Gamma(S_2 > 0) + \bar{\Gamma}(\bar{S}_2 > 0)] + [\Gamma(S_2 < 0) + \bar{\Gamma}(\bar{S}_2 < 0)]} \\ &= -\frac{4}{\pi(\mathcal{D} + \bar{\mathcal{D}})} \int d\omega_1 d\omega_2 k(\omega_1)k(\omega_2)k(\omega_1, \omega_2) \\ &\quad \text{Im}[A_{\perp} A_{\parallel}^* - \bar{A}_{\perp} \bar{A}_{\parallel}^*], \end{aligned} \quad (14)$$

$$\begin{aligned} \mathcal{A}_{T\text{-fake}}^{1,\text{ave}} &\equiv \frac{[\Gamma(S_1 > 0) - \bar{\Gamma}(\bar{S}_1 > 0)] - [\Gamma(S_1 < 0) - \bar{\Gamma}(\bar{S}_1 < 0)]}{[\Gamma(S_1 > 0) + \bar{\Gamma}(\bar{S}_1 > 0)] + [\Gamma(S_1 < 0) + \bar{\Gamma}(\bar{S}_1 < 0)]} \\ &= -\frac{2\sqrt{2}}{\pi(\mathcal{D} + \bar{\mathcal{D}})} \int d\omega_1 d\omega_2 k(\omega_1)k(\omega_2)k(\omega_1, \omega_2) \\ &\quad \text{Im}[A_{\perp} A_0^* + \bar{A}_{\perp} \bar{A}_0^*], \end{aligned} \quad (15)$$

$$\begin{aligned} \mathcal{A}_{T\text{-fake}}^{2,\text{ave}} &\equiv \frac{[\Gamma(S_2 > 0) - \bar{\Gamma}(\bar{S}_2 > 0)] - [\Gamma(S_2 < 0) - \bar{\Gamma}(\bar{S}_2 < 0)]}{[\Gamma(S_2 > 0) + \bar{\Gamma}(\bar{S}_2 > 0)] + [\Gamma(S_2 < 0) + \bar{\Gamma}(\bar{S}_2 < 0)]} \\ &= -\frac{4}{\pi(\mathcal{D} + \bar{\mathcal{D}})} \int d\omega_1 d\omega_2 k(\omega_1)k(\omega_2)k(\omega_1, \omega_2) \\ &\quad \text{Im}[A_{\perp} A_{\parallel}^* + \bar{A}_{\perp} \bar{A}_{\parallel}^*], \end{aligned} \quad (16)$$

with $\bar{\Gamma}$ being the CP -conjugate decay rate, the denominator

$$\bar{D} = \int d\omega_1 d\omega_2 k(\omega_1)k(\omega_2)k(\omega_1, \omega_2) (|\bar{A}_0|^2 + |\bar{A}_\parallel|^2 + |\bar{A}_\perp|^2), \tag{17}$$

and the variables

$$S_1 = \cos \theta_1 \cos \theta_2 \sin \varphi, \quad S_2 = \sin 2\varphi$$

$$\bar{S}_1 = \cos \bar{\theta}_1 \cos \bar{\theta}_2 \sin \bar{\varphi}, \quad \bar{S}_2 = \sin 2\bar{\varphi}. \tag{18}$$

It is shown that $\mathcal{A}_{T\text{-true}}^{1(2),\text{ave}}$ in terms of $\text{Im}[A_\perp A_{0(\parallel)}^* - \bar{A}_\perp \bar{A}_{0(\parallel)}^*]$ is proportional to $\sin \Delta\phi \cos \Delta\delta$. They can be nonzero only in the presence of the weak phase difference $\Delta\phi$. Therefore, the “true” averaged TPAs can provide extra measurements of CP violation. What’s more, compared with the direct CP asymmetries, $\mathcal{A}_{T\text{-true}}^{1(2),\text{ave}}$ does not suffer the suppression from the strong phase difference, which reaches the maximal value when the strong phase difference vanishes. On the contrary, $\mathcal{A}_{T\text{-fake}}^{1(2),\text{ave}} \propto \cos \Delta\phi \sin \Delta\delta$ are not a CP -violating signal as it is nonzero even in the absence of CP -violating phases. Such a quantity will be referred as a “fake” asymmetry (CP conserving), and simply reflects the effect of strong phases [1, 45], instead of CP violation.

In order to make a direct comparison with the future measurements, we also calculate the so-called “true” and “fake” TPAs as follows,

$$\mathcal{A}_{T\text{-true}}^1 = \frac{1}{2}(\mathcal{A}_T^1 + \bar{\mathcal{A}}_T^1)$$

$$= -\frac{\sqrt{2}}{\pi} \int d\omega_1 d\omega_2 k(\omega_1)k(\omega_2)k(\omega_1, \omega_2) \times \text{Im} \left[\frac{A_\perp A_0^*}{\mathcal{D}} - \frac{\bar{A}_\perp \bar{A}_0^*}{\bar{\mathcal{D}}} \right], \tag{19}$$

$$\mathcal{A}_{T\text{-true}}^2 = \frac{1}{2}(\mathcal{A}_T^2 + \bar{\mathcal{A}}_T^2)$$

$$= -\frac{2}{\pi} \int d\omega_1 d\omega_2 k(\omega_1)k(\omega_2)k(\omega_1, \omega_2) \times \text{Im} \left[\frac{A_\perp A_\parallel^*}{\mathcal{D}} - \frac{\bar{A}_\perp \bar{A}_\parallel^*}{\bar{\mathcal{D}}} \right], \tag{20}$$

$$\mathcal{A}_{T\text{-fake}}^1 = \frac{1}{2}(\mathcal{A}_T^1 - \bar{\mathcal{A}}_T^1)$$

$$= -\frac{\sqrt{2}}{\pi} \int d\omega_1 d\omega_2 k(\omega_1)k(\omega_2)k(\omega_1, \omega_2) \times \text{Im} \left[\frac{A_\perp A_0^*}{\mathcal{D}} + \frac{\bar{A}_\perp \bar{A}_0^*}{\bar{\mathcal{D}}} \right], \tag{21}$$

$$\mathcal{A}_{T\text{-fake}}^2 = \frac{1}{2}(\mathcal{A}_T^2 - \bar{\mathcal{A}}_T^2)$$

$$= -\frac{2}{\pi} \int d\omega_1 d\omega_2 k(\omega_1)k(\omega_2)k(\omega_1, \omega_2)$$

$$\times \text{Im} \left[\frac{A_\perp A_\parallel^*}{\mathcal{D}} + \frac{\bar{A}_\perp \bar{A}_\parallel^*}{\bar{\mathcal{D}}} \right], \tag{22}$$

The subscripts “true” and “fake” refer to whether the asymmetry is due to a real CP asymmetry or effects from final-state interactions that are CP symmetric. The two asymmetries defined in Eqs. (13) and (19) are usually different from each other in the most $B_{(s)}$ meson decays, as well as the two asymmetries in Eqs. (14) and (20). They become equal when no direct CP asymmetry occurs in the total decay rate, namely $\mathcal{D} = \bar{\mathcal{D}}$.

3 Perturbative calculation

For simplicity, we will work in the rest frame of the B meson. In the light-cone coordinates, the B meson momentum p_B can be parametrized as $p_B = \frac{m_B}{\sqrt{2}}(1, 1, \mathbf{0}_T)$. Considering the four-body decay $B^0 \rightarrow \rho^0 \phi \rightarrow (\pi^+ \pi^-)(K^+ K^-)$ shown in Fig. 1, we define the intermediate resonance $\rho(\phi)$ with the momentum $p(q)$, and the four final state mesons with the momentum $p_i (i = 1, 4)$, satisfying the momentum conservation relations $p_B = p + q, p = p_1 + p_2, q = p_3 + p_4$. The momentum of the ρ and ϕ can be written as

$$p = \frac{m_B}{\sqrt{2}}(g^+, g^-, \mathbf{0}_T), \quad q = \frac{m_B}{\sqrt{2}}(f^-, f^+, \mathbf{0}_T), \tag{23}$$

in which the factors f^\pm, g^\pm are related to the invariant masses of the meson pairs via $p^2 = \omega_1^2$ and $q^2 = \omega_2^2$,

$$g^\pm = \frac{1}{2} \left[1 + \eta_1 - \eta_2 \pm \sqrt{(1 + \eta_1 - \eta_2)^2 - 4\eta_1} \right],$$

$$f^\pm = \frac{1}{2} \left[1 - \eta_1 + \eta_2 \pm \sqrt{(1 + \eta_1 - \eta_2)^2 - 4\eta_1} \right], \tag{24}$$

with the mass ratio $\eta_{1(2)} = \omega_{1(2)}^2/m_B^2$. The corresponding longitudinal polarization vectors of the P -wave $\pi\pi$ and $K\bar{K}$ pairs can be defined as

$$\epsilon_p = \frac{1}{\sqrt{2}\eta_1}(g^+, -g^-, \mathbf{0}_T), \quad \epsilon_q = \frac{1}{\sqrt{2}\eta_2}(-f^-, f^+, \mathbf{0}_T), \tag{25}$$

which obey the normalization $\epsilon_p^2 = \epsilon_q^2 = -1$ and the orthogonality $\epsilon_p \cdot p = \epsilon_q \cdot q = 0$.

The explicit expressions of the individual momenta p_i can be derived from the relations $p = p_1 + p_2$ and $q = p_3 + p_4$ together with the on-shell conditions $p_i^2 = m_i^2$ for the final state mesons,

$$p_1 = \left(\frac{m_B}{\sqrt{2}} \left(\zeta_1 + \frac{r_1 - r_2}{2\eta_1} \right) g^+, \frac{m_B}{\sqrt{2}} \left(1 - \zeta_1 + \frac{r_1 - r_2}{2\eta_1} \right) g^-, \mathbf{p}_T \right),$$

$$p_2 = \left(\frac{m_B}{\sqrt{2}} \left(1 - \zeta_1 - \frac{r_1 - r_2}{2\eta_1} \right) g^+, \frac{m_B}{\sqrt{2}} \left(\zeta_1 - \frac{r_1 - r_2}{2\eta_1} \right) g^-, -\mathbf{p}_T \right),$$

$$\begin{aligned}
 p_3 &= \left(\frac{m_B}{\sqrt{2}} \left(1 - \zeta_2 + \frac{r_3 - r_4}{2\eta_2} \right) f^-, \frac{m_B}{\sqrt{2}} \left(\zeta_2 + \frac{r_3 - r_4}{2\eta_2} \right) f^+, \mathbf{q}_T \right), \\
 p_4 &= \left(\frac{m_B}{\sqrt{2}} \left(\zeta_2 - \frac{r_3 - r_4}{2\eta_2} \right) f^-, \frac{m_B}{\sqrt{2}} \left(1 - \zeta_2 - \frac{r_3 - r_4}{2\eta_2} \right) f^+, -\mathbf{q}_T \right), \\
 \mathbf{p}_T^2 &= \zeta_1(1 - \zeta_1)\omega_1^2 - \frac{r_1 + r_2}{2\eta_1} + \frac{(r_1 - r_2)^2}{4\eta_1^2}, \\
 \mathbf{q}_T^2 &= \zeta_2(1 - \zeta_2)\omega_2^2 - \frac{r_3 + r_4}{2\eta_2} + \frac{(r_3 - r_4)^2}{4\eta_2^2},
 \end{aligned} \tag{26}$$

with the mass ratios $r_i = m_i^2/m_B^2$, m_i being the masses of the final state mesons, and the term $\zeta_1 + \frac{r_1 - r_2}{2\eta_1} = p_1^+/p^+$ ($\zeta_2 + \frac{r_3 - r_4}{2\eta_2} = p_3^-/q^-$) characterizing the momentum fraction for one of pion-pion (kaon-kaon) pair.

It is easy to obtain the relation between the meson momentum fractions $\zeta_{1,2}$ and the polar angle $\theta_{1,2}$ in the dimension rest frame in Fig. 1,

$$\begin{aligned}
 2\zeta_1 - 1 &= \sqrt{1 + 4\alpha_1} \cos \theta_1, \\
 2\zeta_2 - 1 &= \sqrt{1 + 4\alpha_2} \cos \theta_2,
 \end{aligned} \tag{27}$$

with the two factors

$$\begin{aligned}
 \alpha_1 &= -\frac{r_1 + r_2}{2\eta_1} + \frac{(r_1 - r_2)^2}{4\eta_1^2}, \\
 \alpha_2 &= -\frac{r_3 + r_4}{2\eta_2} + \frac{(r_3 - r_4)^2}{4\eta_2^2},
 \end{aligned} \tag{28}$$

and the bound

$$\begin{aligned}
 \zeta_{1\max,\min} &= \frac{1}{2} \left[1 \pm \sqrt{1 + 4\alpha_1} \right], \\
 \zeta_{2\max,\min} &= \frac{1}{2} \left[1 \pm \sqrt{1 + 4\alpha_2} \right].
 \end{aligned} \tag{29}$$

As illustrated in Fig. 2, there are eight types of Feynman diagrams contributing to the hard kernels H of the four-body decays $B_{(s)} \rightarrow R_1 R_2 \rightarrow (\pi\pi)(KK)$ at leading order in the PQCD approach, which can be classified into three types: the factorizable emission diagrams (Fig. 2a and b); the nonfactorizable emission diagrams (Fig. 2c and d); and the annihilation diagrams (Fig. 2e-h). For the evaluation of the H , we also need to define three valence quark momenta labelled by k_i ($i = B, p, q$) in each meson as

$$\begin{aligned}
 k_B &= (0, x_B p_B^+, \mathbf{k}_{BT}), \quad k_p = (x_1 p^+, 0, \mathbf{k}_{1T}), \\
 k_q &= (0, x_2 q^-, \mathbf{k}_{2T}),
 \end{aligned} \tag{30}$$

with the parton momentum fraction x_i , and the parton transverse momentum \mathbf{k}_{iT} . The small components k_p^- and k_q^+ in Eq. (30) have been dropped in our calculation because k_p and k_q are aligned with the meson pairs in the plus and minus direction. We also neglect the contribution from the k_B^+ component since it does not appear in the hard kernels for dominant factorizable contributions.

In order to calculate the different helicity amplitudes, we first give the weak effective Hamiltonian \mathcal{H}_{eff} of the con-

sidered four-body decays induced by the $b \rightarrow q$ ($q = s, d$) transition,

$$\begin{aligned}
 \mathcal{H}_{eff} &= \frac{G_F}{\sqrt{2}} \left\{ V_{ub} V_{uq}^* \left[C_1(\mu) O_1^u(\mu) + C_2(\mu) O_2^u(\mu) \right] \right. \\
 &\quad \left. - V_{tb} V_{tq}^* \left[\sum_{i=3}^{10} C_i(\mu) O_i(\mu) \right] \right\} + \text{H.c.},
 \end{aligned} \tag{31}$$

with the Fermi constant $G_F = 1.16639 \times 10^{-5} \text{GeV}^{-2}$, Wilson coefficients $C_i(\mu)$ at the renormalization scale μ , the local four-quark operators O_i ($i = 1, \dots, 10$) [75] and the CKM matrix elements V_{ij} .

According to the above Eq. (31), each considered decay channel may receive contributions from one or more terms proportional to different Wilson coefficients C_i . The total decay amplitudes of the $B_{(s)} \rightarrow \rho\phi \rightarrow (\pi\pi)(K\bar{K})$ at LO in the PQCD approach can then be written as

$$\begin{aligned}
 A_h B^+ \rightarrow \rho^+ \phi \rightarrow (\pi^+ \pi^0)(K^+ K^-) \\
 &= -\frac{G_F}{\sqrt{2}} V_{tb}^* V_{td} \left[\left(C_3 + \frac{C_4}{3} + C_5 + \frac{C_6}{3} - \frac{C_7}{2} \right. \right. \\
 &\quad \left. \left. - \frac{C_8}{6} - \frac{C_9}{2} - \frac{C_{10}}{6} \right) F_{ep}^{LL,h} \right. \\
 &\quad \left. + \left(C_4 - \frac{C_{10}}{2} \right) M_{ep}^{LL,h} + \left(C_6 - \frac{C_8}{2} \right) M_{ep}^{SP,h} \right],
 \end{aligned} \tag{32}$$

$$\begin{aligned}
 A_h(B^0 \rightarrow \rho^0 \phi \rightarrow (\pi^+ \pi^-)(K^+ K^-)) \\
 &= -\frac{G_F}{2} V_{tb}^* V_{td} \left[\left(-C_3 - \frac{C_4}{3} - C_5 - \frac{C_6}{3} + \frac{C_7}{2} \right. \right. \\
 &\quad \left. \left. + \frac{C_8}{6} + \frac{C_9}{2} + \frac{C_{10}}{6} \right) F_{ep}^{LL,h} \right. \\
 &\quad \left. - \left(C_4 - \frac{C_{10}}{2} \right) M_{ep}^{LL,h} - \left(C_6 - \frac{C_8}{2} \right) M_{ep}^{SP,h} \right],
 \end{aligned} \tag{33}$$

$$\begin{aligned}
 A_h(B_s^0 \rightarrow \rho^0 \phi \rightarrow (\pi^+ \pi^-)(K^+ K^-)) \\
 &= \frac{G_F}{2} \left\{ V_{ub}^* V_{us} \left[\left(C_1 + \frac{C_2}{3} \right) F_{e\phi}^{LL,h} + C_2 M_{e\phi}^{LL,h} \right] \right. \\
 &\quad \left. - V_{tb}^* V_{ts} \left[\frac{3}{2} \left(C_7 + \frac{C_8}{3} + C_9 + \frac{C_{10}}{3} \right) F_{e\phi}^{LL,h} \right. \right. \\
 &\quad \left. \left. + \frac{3C_{10}}{2} M_{e\phi}^{LL,h} + \frac{3C_8}{2} M_{e\phi}^{SP,h} \right] \right\},
 \end{aligned} \tag{34}$$

with $h = 0, \parallel, \perp$. The individual decay amplitude appeared in the above equations, such as $F_{ep}^{LL,h}$ and $M_{ep}^{LL,h}, M_{ep}^{SP,h}$, is obtained by evaluating the Feynman diagrams in Fig. 2 analytically. The term $F_{ep}^{LL,h}$ ($M_{ep}^{SP,h}$), for example, represents the contribution from the factorizable (nonfactorizable) emission diagrams with $(V-A) \otimes (V-A)$ ($(S-P) \otimes (S+P)$) current. The explicit expressions of $F_{ep}^{LL,h}$ and other decay amplitudes can be found easily in Ref. [69]. The helicity

amplitudes of the S -wave decays have been collected in Appendix A.

As shown in Eq. (1), the DAs of the initial B meson and the final state meson pairs are the most important nonperturbative inputs in the PQCD approach. For the B meson, we adopt the form widely used in the literature [76,77], and more alternative models of the B meson DA and the subleading contributions can be found in Refs. [78–85]. The S - and P -wave two-pion (kaon) DAs, as well as the related time-like form factors are summarized in Appendix B.

4 Numerical analysis

In this section, we work out a number of physical observables for the $B_{(s)} \rightarrow (\pi\pi)(K\bar{K})$ decays, such as the branching ratios, polarization fractions, direct CP asymmetries, together with TPAs. We firstly show the input parameters adopted in our numerical analysis in Table 1, including the decay constants [15,86], the meson masses, the decay widths, the lifetimes and Wolfenstein parameters [87].

The differential branching fraction of the $B_{(s)} \rightarrow (\pi\pi)(K\bar{K})$ in the $B_{(s)}$ meson rest frame can be expressed as:

$$\begin{aligned} & \frac{d^5\mathcal{B}}{d\cos\theta_1 d\cos\theta_2 d\varphi d\omega_1 d\omega_2} \\ &= \frac{\tau_{B_{(s)}} k(\omega_1)k(\omega_2)k(\omega_1, \omega_2)}{16(2\pi)^6 m_{B_{(s)}}^2} |A|^2, \end{aligned} \tag{35}$$

with the $B_{(s)}$ meson lifetime $\tau_{B_{(s)}}$. It has been confirmed that Eq. (35) is equivalent to those in Refs. [88,89] by appropriate variable changes. Replacing the helicity angle $\theta_{1(2)}$ by the meson momentum fraction $\zeta_{1(2)}$ via Eq. (27), the Eq. (35) is turned into

$$\begin{aligned} & \frac{d^5\mathcal{B}}{d\zeta_1 d\zeta_2 d\omega_1 d\omega_2 d\varphi} \\ &= \frac{\tau_{B_{(s)}} k(\omega_1)k(\omega_2)k(\omega_1, \omega_2)}{4(2\pi)^6 m_{B_{(s)}}^2 \sqrt{1+4\alpha_1}\sqrt{1+4\alpha_2}} |A|^2, \end{aligned} \tag{36}$$

where the total decay amplitude A can be written as a coherent sum of the P -, S -, and double S -wave components with $\zeta_{1(2)}$ and φ dependencies

$$\begin{aligned} A &= A_0 \frac{2\zeta_1 - 1}{\sqrt{1+4\alpha_1}} \frac{2\zeta_2 - 1}{\sqrt{1+4\alpha_2}} \\ &+ A_{\parallel} 2\sqrt{2} \sqrt{\frac{\zeta_1(1-\zeta_1) + \alpha_1}{1+4\alpha_1}} \sqrt{\frac{\zeta_2(1-\zeta_2) + \alpha_2}{1+4\alpha_2}} \cos\varphi \\ &+ i A_{\perp} 2\sqrt{2} \sqrt{\frac{\zeta_1(1-\zeta_1) + \alpha_1}{1+4\alpha_1}} \sqrt{\frac{\zeta_2(1-\zeta_2) + \alpha_2}{1+4\alpha_2}} \sin\varphi \\ &+ A_{VS} \frac{2\zeta_1 - 1}{\sqrt{1+4\alpha_1}} + A_{SV} \frac{2\zeta_2 - 1}{\sqrt{1+4\alpha_2}} + A_{SS}. \end{aligned} \tag{37}$$

We can obtain the branching ratio form according to the Eq. (36),

$$\begin{aligned} \mathcal{B}_h &= \frac{\tau_{B_{(s)}}}{4(2\pi)^6 m_{B_{(s)}}^2} \frac{2\pi}{9} C_h \\ &\times \int d\omega_1 d\omega_2 k(\omega_1)k(\omega_2)k(\omega_1, \omega_2) |A_h|^2. \end{aligned} \tag{38}$$

The coefficients C_h are the results of the integrations over $\zeta_1, \zeta_2, \varphi$ in terms of Eq. (38) and listed as follows,

$$C_h = \begin{cases} (1+4\alpha_1)(1+4\alpha_2), & h = 0, \parallel, \perp, \\ 3(1+4\alpha_{1,2}), & h = VS, SV, \\ 9, & h = SS. \end{cases} \tag{39}$$

The CP -averaged branching ratio, the direct CP asymmetries in each component and the overall asymmetry can then be defined as below,

$$\begin{aligned} \mathcal{B}_h^{\text{avg}} &= \frac{1}{2}(\mathcal{B}_h + \bar{\mathcal{B}}_h), \quad \mathcal{A}_h^{\text{dir}} = \frac{\bar{\mathcal{B}}_h - \mathcal{B}_h}{\bar{\mathcal{B}}_h + \mathcal{B}_h}, \\ \mathcal{A}_{CP}^{\text{dir}} &= \frac{\sum_h \bar{\mathcal{B}}_h - \sum_h \mathcal{B}_h}{\sum_h \bar{\mathcal{B}}_h + \sum_h \mathcal{B}_h}, \end{aligned} \tag{40}$$

where $\bar{\mathcal{B}}_h$ is the branching ratio of the corresponding CP -conjugate channel.

For the $B \rightarrow VV$ decays, the additional polarization fractions f_λ with $\lambda = 0, \parallel$, and \perp , are described as

$$f_\lambda = \frac{|A_\lambda|^2}{|A_0|^2 + |A_\parallel|^2 + |A_\perp|^2}, \tag{41}$$

with the normalisation relation $f_0 + f_\parallel + f_\perp = 1$.

4.1 S -wave contributions

The PQCD predictions for the CP -averaged branching ratios of the considered four-body $B_{(s)} \rightarrow [\rho\phi, \rho f_0, f_0\phi, f_0 f_0] \rightarrow (\pi\pi)(K\bar{K})$ decays are summarized in Table 2, in which the theoretical uncertainties are derived from three different sources. The first error results from the parameter of the wave function of the initial state $B_{(s)}$ meson, $\omega_B = 0.40 \pm 0.04$ and $\omega_{B_s} = 0.48 \pm 0.048$ [90–92]. The second one comes from the Gegenbauer moments in the two-meson DAs given in Eq. (B22), and the last one is caused by the variation of the hard scale t from $0.75t$ to $1.25t$ (without changing $1/b_i$) and the QCD scale $\Lambda_{\text{QCD}} = 0.25 \pm 0.05$ GeV, which characterizes the effect of the next-to-leading-order QCD contributions. The three uncertainties are comparable, and their combined impacts could exceed 50%, implying that the nonperturbative parameters in the DAs of the initial and final states need to be constrained more precisely, and the higher-order corrections to four-body B meson decays are critical.

Although the quark model has achieved great successes, the identification of scalar mesons is a long-standing puzzle, and the underlying structure of scalar mesons is not

Table 1 The decay constants are taken from Refs. [15,86]. Other parameters are from PDG 2022 [87]

Wolfenstein parameters	$\lambda = 0.22650$	$A = 0.790$	$\bar{\rho} = 0.141$	$\bar{\eta} = 0.357$
Mass (GeV)	$m_B = 5.28$ $m_{\pi^0} = 0.135$	$m_{B_s} = 5.37$ $m_{K^0} = 0.498$	$m_{\pi^\pm} = 0.140$	$m_{K^\pm} = 0.494$
Decay constants (GeV)	$f_B = 0.21$ $f_\rho = 0.216$	$f_{B_s} = 0.23$ $f_\rho^T = 0.184$	$f_\phi = 0.215$	$f_\phi^T = 0.186$
Decay width (MeV)	$\Gamma_\phi = 4.25$	$\Gamma_\rho = 149.1$		
Lifetime (ps)	$\tau_{B^0} = 1.519$	$\tau_{B^\pm} = 1.638$	$\tau_{B_s} = 1.51$	

Table 2 PQCD predictions for the branching ratios of the $B_{(s)} \rightarrow [VV, VS, SV, SS] \rightarrow (\pi\pi)(K\bar{K})$ decays, with $S = f_0$ and $V = \rho, \phi$. The theoretical uncertainties are attributed to the variations of the shape parameter $\omega_{B_{(s)}}$ in the $B_{(s)}$ meson DA, of the Gegenbauer moments in various twist DAs of $K\bar{K}$ and $\pi\pi$ pairs, and of the hard scale t and the QCD scale Λ_{QCD}

Decay modes	PQCD predictions
$B^+ \rightarrow \rho^+\phi \rightarrow (\pi^+\pi^0)(K^+K^-)$	$(6.40_{-0.98-1.97-0.98}^{+0.98+1.97+0.98}) \times 10^{-8}$
$B^0 \rightarrow \rho^0\phi \rightarrow (\pi^+\pi^-)(K^+K^-)$	$(2.95_{-0.49-0.98-0.49}^{+0.49+0.98+0.49}) \times 10^{-8}$
$B_s^0 \rightarrow \rho^0\phi \rightarrow (\pi^+\pi^-)(K^+K^-)$	$(1.38_{-0.34-0.05-0.15}^{+0.54+0.09+0.15}) \times 10^{-7}$
$B^+ \rightarrow \rho^+f_0 \rightarrow (\pi^+\pi^0)(K^+K^-)$	$(1.25_{-0.45-0.20-0.25}^{+0.59+0.22+0.15}) \times 10^{-7}$
$B^0 \rightarrow \rho^0f_0 \rightarrow (\pi^+\pi^-)(K^+K^-)$	$(3.01_{-0.39-0.95-0.18}^{+0.50+1.34+0.49}) \times 10^{-9}$
$B_s^0 \rightarrow \rho^0f_0 \rightarrow (\pi^+\pi^-)(K^+K^-)$	$(4.01_{-0.76-0.35-0.34}^{+1.08+0.38+0.35}) \times 10^{-9}$
$B^0 \rightarrow f_0\phi \rightarrow (\pi^+\pi^-)(K^+K^-)$	$(0.47_{-0.13-0.24-0.06}^{+0.19+0.20+0.12}) \times 10^{-9}$
$B_s^0 \rightarrow f_0\phi \rightarrow (\pi^+\pi^-)(K^+K^-)$	$(4.09_{-1.58-1.02-1.67}^{+2.24+1.15+1.08}) \times 10^{-7}$
$B^0 \rightarrow f_0f_0 \rightarrow (\pi^+\pi^-)(K^+K^-)$	$(1.93_{-0.67-0.33-0.23}^{+1.05+0.66+0.44}) \times 10^{-10}$
$B_s^0 \rightarrow f_0f_0 \rightarrow (\pi^+\pi^-)(K^+K^-)$	$(7.19_{-2.28-0.60-2.63}^{+4.32+0.71+3.98}) \times 10^{-8}$

well established on the theoretical side (for a review, see Ref. [87]). At present, two main scenarios have been proposed to classify the light scalar resonances [93]. The Scenario-I (S-I) is based on the naive two-quark model, and the light scalar mesons below or near 1 GeV like $f_0(980)$ are regarded as the lowest lying states. While in Scenario-II (S-II), the $f_0(980)$ is identified as the predominant four-quark state $q^2\bar{q}^2$, and the scalars above 1 GeV are treated as the ground $q\bar{q}$ states. Since it is difficult for us to study these S-wave decays based on the four-quark picture, we shall consider the conventional $q\bar{q}$ assignment for the light scalar $f_0(980)$ to give several quantitative predictions. In Scenario-I, $f_0(980)$ is mainly treated as an $s\bar{s}$ state, which has been supported by $D_s^+ \rightarrow f_0\pi, \phi \rightarrow f_0\gamma$ decays [87]. However, there also exists some experimental evidences indicating that $f_0(980)$ is not purely an $s\bar{s}$ state. For example, the observation of $\Gamma(J/\psi \rightarrow f_0\omega) \simeq \frac{1}{2}\Gamma(J/\psi \rightarrow f_0\phi)$ [87] clearly shows the existence of the non-strange and strange quark content. Therefore, $f_0(980)$ should be a mixture of

$$n\bar{n} = \frac{1}{\sqrt{2}}(u\bar{u} + d\bar{d}) \text{ and } s\bar{s},$$

$$|f_0\rangle = |n\bar{n}\rangle\sin\theta + |s\bar{s}\rangle\cos\theta. \tag{42}$$

The value of the mixing angle θ in the above equation has not been determined precisely so far, which is suggested to be in the wide ranges of $25^\circ < \theta < 40^\circ$ and $140^\circ < \theta < 165^\circ$ [94–96]. For simplicity, we will adopt the value $\theta = 145^\circ$ [20,97] in our calculation. In our previous works [69–72], the scalar meson $f_0(980)$ is usually considered as the pure $s\bar{s}$ state. Furthermore, there also exist some theoretical studies on the $B_{(s)}$ meson decays involving $f_0(980)$ in the final states based on the assumption that $f_0(980)$ is a pure $s\bar{s}$ density operator [98–100]. In Ref. [73], on the other hand, we found that the contribution from the $f_0 = (u\bar{u} + d\bar{d})/\sqrt{2}$ component is significant in the decays like $B^0 \rightarrow \rho^0f_0$ governed by $B \rightarrow f_n$ transition form factor. Thus, the mixing effect shown in Eq. (42) should also be taken into account in this work.

The two-body branching ratio $\mathcal{B}(B_{(s)} \rightarrow R_1R_2)$ can usually be extracted from the corresponding four-body decay modes in Table 2 under the narrow width approximation:

$$\mathcal{B}(B_{(s)} \rightarrow R_1R_2 \rightarrow (\pi\pi)(K\bar{K})) \approx \mathcal{B}(B_{(s)} \rightarrow R_1R_2) \times \mathcal{B}(R_1 \rightarrow \pi\pi) \times \mathcal{B}(R_2 \rightarrow K\bar{K}). \tag{43}$$

The \mathcal{B} of the three-body decay $B^0 \rightarrow \rho^0(f_0 \rightarrow)\pi^+\pi^-$ can then be calculated as follows:

$$\mathcal{B}(B^0 \rightarrow \rho^0(f_0 \rightarrow)\pi^+\pi^-) = \frac{\mathcal{B}(B^0 \rightarrow \rho^0f_0 \rightarrow (\pi^+\pi^-)(K^+K^-))}{\mathcal{B}(\rho^0 \rightarrow \pi^+\pi^-)}.$$

$$R_{\pi/K} = (0.09_{-0.03}^{+0.05}) \times 10^{-7}, \tag{44}$$

with the ratio $R_{\pi/K} = \frac{\mathcal{B}(f_0 \rightarrow \pi^+\pi^-)}{\mathcal{B}(f_0 \rightarrow K^+K^-)}$. Recent years, BABAR [101] and BES [102,103] Collaborations have performed systematically measurements on the ratio of the partial decay width of $f_0 \rightarrow K^+K^-$ to $f_0 \rightarrow \pi^+\pi^-$,

$$R_{K/\pi}^{\text{exp}} = \begin{cases} 0.69 \pm 0.32 & \text{BABAR,} \\ 0.25_{-0.11}^{+0.17} & \text{BES,} \end{cases} \tag{45}$$

and we have adopted their average value $R_{K/\pi}^{\text{exp}} = 0.35 \pm 0.11$ [104] in Eq. (44). The $B^0 \rightarrow \rho^0f_0$ decay mode has

also been studied in the two-body framework within the PQCD [18] and QCDF [7] approaches. In the narrow-width limit, one can get the following branching fractions

$$\begin{aligned} &\mathcal{B}(B^0 \rightarrow \rho^0(f_0 \rightarrow) \pi^+ \pi^-) \\ &= \begin{cases} (0.10_{-0.00}^{+0.15}) \times 10^{-7} \text{ QCDF,} \\ (1.65_{-0.84}^{+1.00}) \times 10^{-7} \text{ PQCD,} \end{cases} \end{aligned} \tag{46}$$

where $\mathcal{B}(f_0 \rightarrow \pi^+ \pi^-) = 0.5$ [7] is used. Our calculation $\mathcal{B} = (0.09_{-0.03}^{+0.05}) \times 10^{-7}$ is consistent well with the QCDF prediction [7], but far from the previous PQCD value [18]. It should be noted that, strictly speaking, the narrow width approximation has not been fully justified since such approximation has its scope of application. Specially for the broad scalar intermediate states like $f_0(980)$, the narrow-width approximation should be corrected by including the finite-width effects [105, 106]. We can then only make a rough estimate of $\mathcal{B}(B^0 \rightarrow \rho^0(f_0 \rightarrow) \pi^+ \pi^-)$ from the previous two-body results according to Eq. (43) at present. Nonetheless, all these theoretical predictions are much smaller than the current experimental data $\mathcal{B}^{\text{exp}} = (7.8 \pm 2.5) \times 10^{-7}$ [87], which may be clarified in the following form. First, the $B^0 \rightarrow \rho^0(f_0 \rightarrow) \pi^+ \pi^-$ decay is ascribed to the involved color suppressed tree contributions. Since only leading order diagrams have been concerned in the current work, it indicates that this decay might receive substantial next-to-leading-order (NLO) corrections. Besides, as shown in Ref. [73], the calculated \mathcal{B} of the decay $B^0 \rightarrow f_0 \rho^0$ is sensitive to the Gegenbauer moment a_S and the mixing angle θ . It is expected that maybe we can fit the related non-perturbative parameters with abundant data to match the experiment when NLO corrections to four-body decays in the PQCD framework are considered, which goes beyond the scope of the present work and should be left for the future studies.

We remark that the $K\bar{K}$ invariant mass of the S -wave decays has been limited in a narrow window of ± 30 MeV around the known ϕ mass in this study. As claimed in Refs. [71, 72], the contribution of scalar resonance $f_0(980)$ relies on the final-state invariant mass range strongly, since it has a wide decay width. We have recalculated the \mathcal{B} of the decay $B^0 \rightarrow \rho^0 f_0 \rightarrow (\pi^+ \pi^-)(K^+ K^-)$ by enlarging the S -wave $K\bar{K}$ invariant mass range from $[m_\phi - 30\text{MeV}, m_\phi + 30\text{MeV}]$ to $[2m_K, m_B - m_\rho]$: $\mathcal{B} = 2.95 \times 10^{-8}$. The corresponding branching fraction of the three-body decay $B^0 \rightarrow \rho^0(f_0 \rightarrow) \pi^+ \pi^-$ is then estimated to be 0.84×10^{-7} , which is larger than the value in Eq. (44) by almost one order. In addition, due to the finite-width effects of the scalar resonance $f_0(980)$ as mentioned previously, the result $\mathcal{B} = (0.09_{-0.03}^{+0.05}) \times 10^{-7}$ evaluated from the $\mathcal{B}(B^0 \rightarrow \rho^0 f_0 \rightarrow (\pi^+ \pi^-)(K^+ K^-))$ may suffer from a large uncertainty. Therefore, we hope that the future experiments can perform a direct measurement on the four-body decay $B^0 \rightarrow \rho^0 f_0 \rightarrow (\pi^+ \pi^-)(K^+ K^-)$.

Relying on the fraction $\mathcal{B}(\phi \rightarrow K^+ K^-) = 49.2\%$ [87], we can extract the $\mathcal{B}(B_s^0 \rightarrow \phi(f_0 \rightarrow) \pi^+ \pi^-)$ from the four-body decay $B_s^0 \rightarrow f_0 \phi \rightarrow (\pi^+ \pi^-)(K^+ K^-)$ in Table 2 under the narrow width limit:

$$\begin{aligned} &\mathcal{B}(B_s^0 \rightarrow \phi(f_0 \rightarrow) \pi^+ \pi^-) \\ &= \frac{\mathcal{B}(B_s^0 \rightarrow f_0 \phi \rightarrow (\pi^+ \pi^-)(K^+ K^-))}{\mathcal{B}(\phi \rightarrow K^+ K^-)} \\ &= (0.83_{-0.51}^{+0.54}) \times 10^{-6}. \end{aligned} \tag{47}$$

Although the above theoretical central value is a bit smaller than the experimental data $\mathcal{B}^{\text{exp}} = (1.12 \pm 0.21) \times 10^{-6}$ [87], our result can still accommodate the current measurement with large uncertainties, and also comparable with the previous three-body PQCD result [107]. In Ref. [20], the authors have studied the branching fraction of the two-body decay $B_s^0 \rightarrow \phi f_0$ in PQCD approach, and one can obtain $\mathcal{B}(B_s^0 \rightarrow \phi(f_0 \rightarrow) \pi^+ \pi^-) = (0.24_{-0.14}^{+0.21}) \times 10^{-6}$ according to Eq. (43). It is shown that our calculation $\mathcal{B} = (0.83_{-0.51}^{+0.54}) \times 10^{-6}$ presented in Eq. (47) is a bit larger than the converted value $(0.24_{-0.14}^{+0.21}) \times 10^{-6}$ [20] from the previous two-body PQCD result by a factor of ~ 3 , but more close to the experimental data. As already stressed previously that in fact the narrow width approximation is not exactly valid for the broad intermediate states like $f_0(980)$. For these resonances, the finite-width effects is significant and should be considered. Thus, the above comparisons is just a rough estimate for a cross-checking. Overall, since the property of the scalar resonance $f_0(980)$ is not well understood, and both the theoretical and experimental uncertainties are relatively large, all the above issues need to be further clarified in the future.

4.2 Branching ratios and polarization fractions of two-body $B_{(S)} \rightarrow \rho\phi$ decays

On basis of the narrow width approximation Eq. (43), the branching ratios of the two-body decays $B_{(S)} \rightarrow \rho\phi$ have been extracted in Table 3. The polarization fractions f_i ($i = 0, \parallel, \perp$) of the two-body $B_{(S)} \rightarrow \rho\phi$ decays calculated in this work have also been listed in Table 3. For a comparison, the updated predictions in the QCDF [5], the previous predictions in the PQCD approach [23], SCET [30] and FAT [31] are also displayed in Table 3, and the experimental results for branching ratios are taken from PDG 2022 [87].

Most of the theoretical predictions of $\mathcal{B}(B_s^0 \rightarrow \rho^0 \phi)$ agree well with the current data within errors. The calculated branching ratio $(0.28_{-0.07}^{+0.12}) \times 10^{-6}$ of the decay $B_s^0 \rightarrow \rho^0 \phi$ is much smaller than those of other $b \rightarrow s$ transition processes, such as $B_s^0 \rightarrow K^* K^*$ decays. To see clearly the contributions from different topology diagrams, we show the explicit numerical results of the $B_s^0 \rightarrow \rho^0 \phi$ decay in Table 4, in which we just quote the central values. We know that $|V_{tb}^* V_{ts}|$ and

Table 3 Branching ratios and polarization fractions of the two-body $B_{(s)} \rightarrow \rho\phi$ decays. For a comparison, we also list the results from the previous PQCD [23], QCDF [5], SCET [30], and FAT [31]. The world averages of experimental data are taken from PDG 2022 [87]. The sources of the theoretical errors are the same as in Table 2

Modes	$\mathcal{B}(10^{-6})$	$f_0(\%)$	$f_{\parallel}(\%)$	$f_{\perp}(\%)$
$B_s^0 \rightarrow \rho^0\phi$	$0.28^{+0.11+0.02+0.03}_{-0.07-0.01-0.02}$	$86.58^{+0.25+0.56+0.46}_{-0.13-0.52-0.19}$	$6.45^{+0.05+0.27+0.09}_{-0.11-0.26-0.17}$	$6.98^{+0.07+0.30+0.11}_{-0.14-0.30-0.24}$
PQCD [23]	$0.23^{+0.15}_{-0.05}$	86 ± 1	...	$8.89^{+0.80}_{-1.06}$
QCDF [5]	$0.18^{+0.09}_{-0.04}$	88^{+2}_{-18}
SCET [30]	0.36 ± 0.05	100
FAT [31]	0.07 ± 0.03
Data [87]	0.27 ± 0.08
$B^0 \rightarrow \rho^0\phi$	$0.006^{+0.001+0.002+0.001}_{-0.001-0.002-0.001}$	$85.47^{+0.00+3.95+4.26}_{-0.46-6.52-6.46}$	$7.73^{+0.25+3.46+4.36}_{-0.06-2.10-3.08}$	$6.80^{+0.21+3.04+2.06}_{-0.00-1.86-1.19}$
PQCD [23]	$0.013^{+0.007}_{-0.006}$	95 ± 1	...	$2.36^{+1.08}_{-0.76}$
SCET [30]	≈ 0.002	100
FAT [31]	0.03 ± 0.01
Data [87]	< 0.33
$B^+ \rightarrow \rho^+\phi$	$0.013^{+0.002+0.004+0.002}_{-0.002-0.004-0.002}$	$85.47^{+0.00+3.95+4.26}_{-0.46-6.52-6.46}$	$7.73^{+0.25+3.46+4.36}_{-0.06-2.10-3.08}$	$6.80^{+0.21+3.04+2.06}_{-0.00-1.86-1.19}$
PQCD [23]	$0.028^{+0.015}_{-0.013}$	95^{+1}_{-2}	...	$2.36^{+1.08}_{-0.76}$
SCET [30]	0.005 ± 0.001	100
FAT [31]	0.06 ± 0.02
Data [87]	< 3.0

Table 4 Branching ratios of the four-body decay $B_s^0 \rightarrow \rho^0\phi \rightarrow (\pi^+\pi^-)(K^+K^-)$ from different topology diagrams. FE and NFE represent the contributions from factorizable emission and nonfactorizable emission diagrams, respectively

Channel	Tree $\mathcal{B}(10^{-6})$			Penguin $\mathcal{B}(10^{-6})$		
	FE	NFE	Total	FE	NFE	Total
$B_s^0 \rightarrow \rho^0\phi \rightarrow (\pi^+\pi^-)(K^+K^-)$	0.013	0.018	0.031	0.214	0.001	0.215

$|V_{ub}^* V_{us}|$ are $\mathcal{O}(\lambda^2)$ and $\mathcal{O}(\lambda^4)$ respectively, with $\lambda \sim 0.22$. This implies that the tree operators of the $b \rightarrow s$ transition decays like $B_s^0 \rightarrow \rho^0\phi$ are highly suppressed by the CKM matrix elements $|V_{ub}^* V_{us}|$. Furthermore, the tree amplitudes of the $B_s^0 \rightarrow \rho^0\phi$ channel in the factorizable emission diagrams Fig. 2a and b are also suppressed by the small Wilson coefficients $C_1 + C_2/3$. The dominant contributions are then from the penguin operators. However as show in Eq. (34), the $B_s^0 \rightarrow \rho^0\phi$ decay has no gluonic penguin amplitudes because of the cancellations between the $u\bar{u}$ and $d\bar{d}$ component in the ρ^0 meson. The only left parts are all electroweak penguin suppressed. As a result, the total branching ratio of the $B_s^0 \rightarrow \rho^0\phi$ is estimated to be small, at the order of 10^{-7} .

For other two $B^0 \rightarrow \rho^0\phi$ and $B^+ \rightarrow \rho^+\phi$ decay channels controlled by $b \rightarrow d$ transitions, the predicted branching ratios are much smaller than that of $B_s^0 \rightarrow \rho^0\phi$ decay due to the CKM-suppressed factor $|V_{td}/V_{ts}|^2 \sim 0.05$. The calculated $\mathcal{B}(B^+ \rightarrow \rho^+\phi) = (0.013 \pm 0.005) \times 10^{-6}$ and $\mathcal{B}(B^0 \rightarrow \rho^0\phi) = (0.006 \pm 0.002) \times 10^{-6}$ in this work are about half of the previous two-body results $\mathcal{B}(B^+ \rightarrow \rho^+\phi) = (0.028^{+0.015}_{-0.013}) \times 10^{-6}$ [23] and $\mathcal{B}(B^0 \rightarrow \rho^0\phi) =$

$(0.013^{+0.007}_{-0.006}) \times 10^{-6}$ [23]. The main reason is that the additional higher power corrections related to the momenta fraction x_B have been taken into account in the current work, which has been ignored in Ref. [23]. Taking the $B^0 \rightarrow \rho^0\phi$ decay as an example, we have reexamined the branching fraction without the contributions from x_B : $\mathcal{B}(B^0 \rightarrow \rho^0\phi) = 0.01 \times 10^{-6}$, which becomes similar to the previous two-body analysis. The current experiments give the upper limits: $\mathcal{B}(B^+ \rightarrow \rho^+\phi) < 3.0 \times 10^{-6}$ [87] and $\mathcal{B}(B^0 \rightarrow \rho^0\phi) < 3.3 \times 10^{-7}$ [87] at 90% C.L, so more precise measurements are expected to differentiate these theoretical predictions. Besides, under the isospin limit the following relation among the $B^0 \rightarrow \rho^0\phi$ and $B^+ \rightarrow \rho^+\phi$ decays is naively expected

$$R = \frac{\mathcal{B}(B^0 \rightarrow \rho^0\phi)}{\mathcal{B}(B^+ \rightarrow \rho^+\phi)} \approx \frac{1}{2} \cdot \frac{\tau_{B^0}}{\tau_{B^+}}. \quad (48)$$

Our calculations basically agree with the relation given above and can be tested by the future experiments.

In the naive factorization approach, the longitudinal polarizations are expected to dominate the branching ratios of

charmless $B \rightarrow VV$ decays according to the naive counting rules [9]

$$f_0 \sim 1 - \mathcal{O}(m_V^2/m_B^2), \quad f_{\parallel} \sim f_{\perp} \sim \mathcal{O}(m_V^2/m_B^2), \quad (49)$$

with m_V being the vector meson mass. In sharp contrast to these expectations, large transverse polarization of order 50% is observed in the penguin dominated decays $B \rightarrow K^*\rho$, $B \rightarrow K^*\phi$, and $B_s^0 \rightarrow \phi\phi$ [34, 35, 39, 54–56], which reflects that the counting rules given in Eq. (49) is violated and poses an interesting challenge for the theory. In order to interpret this large transverse polarization, a number of strategies have been proposed within or beyond the SM [2, 25, 108–129]. In the PQCD approach, the unexpected large transverse components are led by the penguin annihilation diagrams, especially the $(S - P)(S + P)$ penguin annihilation, introduced by the QCD penguin operator O_6 [108], which is originally introduced in Ref. [130].

For the $B^0 \rightarrow \rho^0\phi$, $B^+ \rightarrow \rho^+\phi$ and $B_s^0 \rightarrow \rho^0\phi$ decays, the longitudinal polarization fractions are predicted to be as large as 90%, which agree well with the previous PQCD calculations [15, 23] and those from QCDF [5], SCET [30] and FAT [31] within uncertainties. The $B_{(s)} \rightarrow \rho\phi$ are pure emission-type decays, and the contributions from the chirally enhanced $(S - P)(S + P)$ penguin annihilation operator vanishes. Besides taking the $B_s^0 \rightarrow \rho^0\phi$ decay as an example, the dominant contributions are from the $3/2[C_7 + C_8/3 + C_9 + C_{10}/3]F_{e\phi}^{LL,h}$ ($h = 0, \parallel, \perp$) induced by the electroweak penguin operators in the factorizable emission diagrams. Compared with the longitudinal component $F_{e\phi}^{LL,0}$, the transverse amplitudes $F_{e\phi}^{LL,\parallel}$ and $F_{e\phi}^{LL,\perp}$ are always highly suppressed by the factor $\omega_{\pi\pi}/m_{B_s} \approx m_{\rho}/m_{B_s} \approx 0.02$, which leads to $f_0 \sim 90\%$.

4.3 CP-violating observables

The direct CP asymmetries with each helicity state ($\mathcal{A}_{0,\parallel,\perp}^{\text{CP}}$) of the four-body $B_s^0 \rightarrow \rho^0\phi \rightarrow (\pi^+\pi^-)(K^+K^-)$ decay together with those summed over all helicity states ($\mathcal{A}_{\text{dir}}^{\text{CP}}$) are listed in Table 5. For comparison, we also present the updated results of the QCDF [5], SCET [30], FAT [31], and the PQCD [23] predictions in two-body framework. Meanwhile, the direct CP asymmetry \mathcal{A}^{CP} of the S-wave decays $B_{(s)} \rightarrow [VS, SV, SS] \rightarrow (\pi\pi)(K\bar{K})$ are also displayed in Table 6. The kinematics of the two-body decays is fixed, while the amplitudes of the quasi-two-body decays depend on the invariant mass of the final-state pairs, resulting in the differential distribution of direct CP asymmetries. The CP asymmetry in the four-body framework is moderated by the finite width of the intermediate resonance appearing in the time-like form factor $F(\omega^2)$. Hence, it is reasonable to see the differences of direct CP asymmetries between the two-

body and four-body frameworks in the PQCD approach as shown in Table 5.

The direct CP asymmetries of the two $\bar{b} \rightarrow \bar{d}\bar{s}s$ transition decays $B^0 \rightarrow \rho^0\phi \rightarrow (\pi^+\pi^-)(K^+K^-)$ and $B^+ \rightarrow \rho^+\phi \rightarrow (\pi^+\pi^0)(K^+K^-)$ are naturally expected to be zero since only penguin operators work on these decays. However, the $B_s^0 \rightarrow \rho^0\phi \rightarrow (\pi^+\pi^-)(K^+K^-)$ mode receives the additional tree contributions, and the interference between the tree and penguin amplitudes leads to the direct CP asymmetry: $\mathcal{A}_{\text{dir}}^{\text{CP}} = (21.8_{-3.3}^{+2.7})\%$. For the S-wave decays shown in Table 6, it is interesting to see that the predicted \mathcal{A}^{CP} of the two double S-wave decays $B^0 \rightarrow f_0f_0 \rightarrow (\pi^+\pi^-)(K^+K^-)$ and $B_s^0 \rightarrow f_0f_0 \rightarrow (\pi^+\pi^-)(K^+K^-)$ are indeed quite different. As can be seen from the related numerical results in Table 7, the fact is that for the $B_s^0 \rightarrow f_0f_0 \rightarrow (\pi^+\pi^-)(K^+K^-)$ decay, the tree operators are highly suppressed by the CKM matrix elements $|V_{us}V_{ub}^*|$, in comparison with $|V_{ts}V_{tb}^*|$ related to the penguin operators. For $B^0 \rightarrow f_0f_0 \rightarrow (\pi^+\pi^-)(K^+K^-)$ decay, both of $|V_{ud}V_{ub}^*|$ and $|V_{td}V_{tb}^*|$ are in the same order (10^{-3}), which can strengthen the interference between the tree and penguin amplitudes. Therefore, the predicted \mathcal{A}^{CP} of the $B_s^0 \rightarrow f_0f_0 \rightarrow (\pi^+\pi^-)(K^+K^-)$ is much smaller than that of the $B^0 \rightarrow f_0f_0 \rightarrow (\pi^+\pi^-)(K^+K^-)$ decay. Besides, we have added two more figures in Fig. 3 to illustrate the above clarifications. In Fig. 3a, we plot the differential distribution of $\frac{d^2B(B^0 \rightarrow f_0f_0 \rightarrow (\pi^+\pi^-)(K^+K^-))}{d\omega_1 d\omega_2}$ in the ω_1 - ω_2 plane to show the contributions from the intermediate resonances. While in Fig. 3b, we display the differential distribution of $\mathcal{A}^{\text{CP}}(B^0 \rightarrow f_0f_0 \rightarrow (\pi^+\pi^-)(K^+K^-))$ in the ω_1 - ω_2 plane to show the regional CP asymmetries. One can see that, in general, the direct CP asymmetries are significant in the region around the pole mass of the intermediate resonance.

As it is known that the direct CP asymmetry depends on both the strong phase and the weak CKM phase. In the SCET, the large strong phase is only from the long-distance charming penguin at leading power and leading order. In the QCDF and PQCD approaches, the strong phase comes from the hard spectator scattering and annihilation diagrams respectively. So, the origins of strong phase are actually different in these three approaches, which leads to different predictions of $\mathcal{A}_{\text{dir}}^{\text{CP}}(B_s^0 \rightarrow \rho^0\phi)$. The forthcoming LHCb and Belle-II measurements for the direct CP asymmetries can help us to examine these factorization approaches. The PQCD predictions for the “true” and “fake” TPAs of the $B_{(s)} \rightarrow \rho\phi \rightarrow (\pi\pi)(K\bar{K})$ decays are collected in Table 8. As mentioned previously, the averaged asymmetries $\mathcal{A}_{\text{T-true}}^{1(2),\text{ave}}$ ($\mathcal{A}_{\text{T-fake}}^{1(2),\text{ave}}$) are usually not equal to the so-called “true” (“fake”) asymmetries $\mathcal{A}_{\text{T-true}}^{1(2)}$ ($\mathcal{A}_{\text{T-fake}}^{1(2)}$). They become equal only in the absence of direct CP violation in the total rates, namely $\mathcal{D} = \bar{\mathcal{D}}$, such as the $B^0 \rightarrow \rho^0\phi \rightarrow$

Table 5 Direct CP asymmetries (in units of %) for the $B_s^0 \rightarrow \rho^0 \phi \rightarrow (\pi^+ \pi^-)(K^+ K^-)$ decay compared with the previous predictions in the PQCD approach [23], the updated predictions in the QCDF [5],

SCET [30] and FAT [31]. The sources of the theoretical errors are the same as in Table 2

Modes	$\mathcal{A}_0^{\text{CP}}$	$\mathcal{A}_{\parallel}^{\text{CP}}$	$\mathcal{A}_{\perp}^{\text{CP}}$	$\mathcal{A}_{\text{dir}}^{\text{CP}}$
$B_s^0 \rightarrow \rho^0 \phi \rightarrow (\pi^+ \pi^-)(K^+ K^-)$	$29.4^{+0.4+0.9+2.9}_{-0.1-1.0-3.8}$	$-27.7^{+0.8+0.5+5.2}_{-1.1-0.4-5.6}$	$-26.6^{+0.7+0.6+4.7}_{-1.0-0.5-4.9}$	$21.8^{+0.6+1.1+2.4}_{-0.1-1.1-3.1}$
PQCD [23]	$3.27^{+1.07}_{-1.19}$		$-32.8^{+7.4}_{-5.8}$	$-4.3^{+1.5}_{-1.2}$
QCDF [5]	83^{+10}_{-36}
SCET [30]	0
FAT [31]	0

Table 6 PQCD predictions for the direct CP asymmetries \mathcal{A}^{CP} (in units of %) of the $B_{(s)} \rightarrow [VS, SV, SS] \rightarrow (\pi\pi)(K\bar{K})$ decays, with $S = f_0(980)$ and $V = \rho, \phi$. The sources of the theoretical errors are the same as in Table 2

Decay modes	PQCD predictions
$B^+ \rightarrow \rho^+ f_0 \rightarrow (\pi^+ \pi^0)(K^+ K^-)$	$-8.8^{+0.8+1.2+0.9}_{-0.9-0.8-0.9}$
$B^0 \rightarrow \rho^0 f_0 \rightarrow (\pi^+ \pi^-)(K^+ K^-)$	$-17.6^{+0.0+13.7+26.2}_{-6.2-14.9-23.4}$
$B_s^0 \rightarrow \rho^0 f_0 \rightarrow (\pi^+ \pi^-)(K^+ K^-)$	$21.3^{+1.4+3.3+2.9}_{-0.6-3.9-3.8}$
$B^0 \rightarrow f_0 \phi \rightarrow (\pi^+ \pi^-)(K^+ K^-)$	0.0
$B_s^0 \rightarrow f_0 \phi \rightarrow (\pi^+ \pi^-)(K^+ K^-)$	$5.4^{+2.9+3.9+1.6}_{-0.0-2.0-4.8}$
$B^0 \rightarrow f_0 f_0 \rightarrow (\pi^+ \pi^-)(K^+ K^-)$	$-79.4^{+7.7+25.3+4.4}_{-2.2-1.1-2.3}$
$B_s^0 \rightarrow f_0 f_0 \rightarrow (\pi^+ \pi^-)(K^+ K^-)$	$-0.06^{+0.00+0.00+0.00}_{-3.41-5.50-3.22}$

Table 7 Branching ratios of the double S -wave four-body decays $B^0 \rightarrow f_0 f_0 \rightarrow (\pi^+ \pi^-)(K^+ K^-)$ and $B_s^0 \rightarrow f_0 f_0 \rightarrow (\pi^+ \pi^-)(K^+ K^-)$ from different topology diagrams

Decay modes	Tree contributions	Penguin contributions
$B^0 \rightarrow f_0 f_0 \rightarrow (\pi^+ \pi^-)(K^+ K^-)$	0.78×10^{-10}	1.12×10^{-10}
$B_s^0 \rightarrow f_0 f_0 \rightarrow (\pi^+ \pi^-)(K^+ K^-)$	2.22×10^{-11}	7.12×10^{-8}

$(\pi^+ \pi^-)(K^+ K^-)$ and $B^+ \rightarrow \rho^+ \phi \rightarrow (\pi^+ \pi^0)(K^+ K^-)$ decays.

For the two pure penguin decays $B^0 \rightarrow \rho^0 \phi \rightarrow (\pi^+ \pi^-)(K^+ K^-)$ and $B^+ \rightarrow \rho^+ \phi \rightarrow (\pi^+ \pi^0)(K^+ K^-)$, each helicity amplitude involves the same single weak phase in the SM, resulting in $A_{\mathcal{T}}^i = -\bar{A}_{\mathcal{T}}^i$ due to the vanish-

ing weak phase difference. The “true” TPAs for these two decay channels are thus expected to be zero. If such asymmetries are observed experimentally, it is probably a signal of new physics. However, since the $B_s^0 \rightarrow \rho^0 \phi \rightarrow (\pi^+ \pi^-)(K^+ K^-)$ decay can receive extra tree contributions, the magnitude of the calculated “true” TPA can exceed ten percent, which is expected to be tested by the future experiments. As “fake” TPAs are due to strong phases and require no weak phase difference, the predicted $\mathcal{A}_{\mathcal{T}\text{-fake}}^{1(2)}$ and $\mathcal{A}_{\mathcal{T}\text{-fake}}^{1(2),\text{ave}}$ are usually nonzero for all considered decays. The predicted large “fake” asymmetry $\mathcal{A}_{\mathcal{T}\text{-fake}}^1 =$

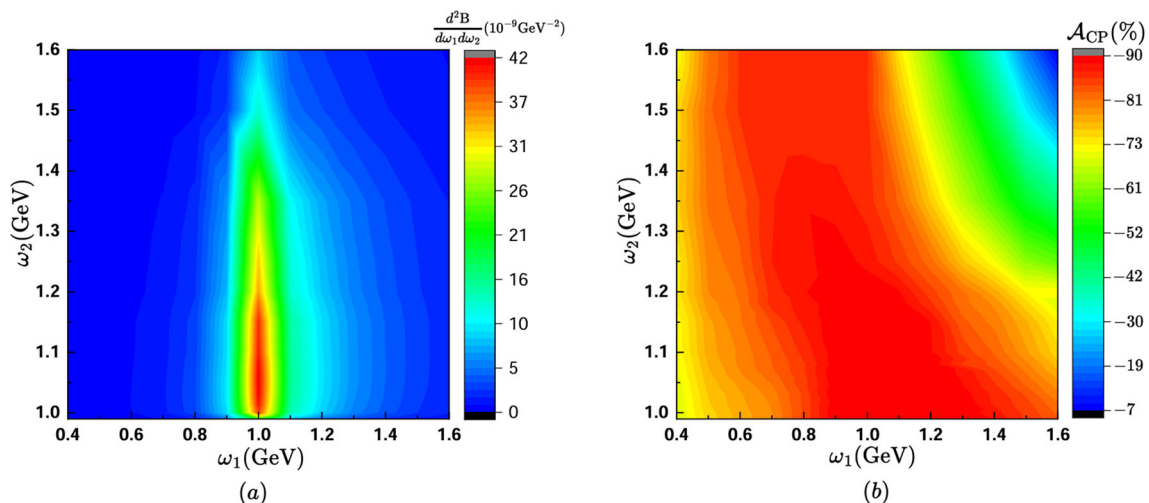


Fig. 3 (a) Differential branching ratio $\frac{d^2 B}{d\omega_1 d\omega_2}$ and (b) the regional CP asymmetries \mathcal{A}^{CP} of the $B^0 \rightarrow f_0 f_0 \rightarrow (\pi^+ \pi^-)(K^+ K^-)$ decay in the ω_1 - ω_2 plane

Table 8 PQCD predictions for the TPAs (%) of the four-body $B_{(s)} \rightarrow \rho\phi \rightarrow (\pi\pi)(K\bar{K})$ decays. The sources of theoretical errors are the same as in Table 2 but added in quadrature

Modes	TPAs-1					
	\mathcal{A}_T^1	$\bar{\mathcal{A}}_T^1$	$\mathcal{A}_{T\text{-true}}^1$	$\mathcal{A}_{T\text{-fake}}^1$	$\mathcal{A}_{T\text{-True}}^{(1)\text{ave}}$	$\mathcal{A}_{T\text{-fake}}^{(1)\text{ave}}$
$B^+ \rightarrow \rho^+\phi \rightarrow (\pi^+\pi^0)(K^+K^-)$	$-20.92^{+6.26}_{-2.80}$	$20.92^{+2.80}_{-6.26}$	0	$-20.92^{+6.26}_{-2.80}$	0	$-20.92^{+6.26}_{-2.80}$
$B^0 \rightarrow \rho^0\phi \rightarrow (\pi^+\pi^-)(K^+K^-)$	$-20.92^{+6.26}_{-2.80}$	$20.92^{+2.80}_{-6.26}$	0	$-20.92^{+6.26}_{-2.80}$	0	$-20.92^{+6.26}_{-2.80}$
$B_s^0 \rightarrow \rho^0\phi \rightarrow (\pi^+\pi^-)(K^+K^-)$	$-23.53^{+1.05}_{-0.62}$	$3.06^{+3.22}_{-3.11}$	$-10.23^{+1.73}_{-1.56}$	$-13.29^{+1.79}_{-1.45}$	$-11.42^{+1.82}_{-1.58}$	$-14.20^{+1.51}_{-1.25}$
Modes	TPAs-2					
	\mathcal{A}_T^2	$\bar{\mathcal{A}}_T^2$	$\mathcal{A}_{T\text{-true}}^2$	$\mathcal{A}_{T\text{-fake}}^2$	$\mathcal{A}_{T\text{-True}}^{(2)\text{ave}}$	$\mathcal{A}_{T\text{-fake}}^{(2)\text{ave}}$
$B^+ \rightarrow \rho^+\phi \rightarrow (\pi^+\pi^0)(K^+K^-)$	$1.02^{+1.12}_{-0.54}$	$-1.02^{+1.12}_{-0.54}$	0	$1.02^{+1.12}_{-0.54}$	0	$1.02^{+1.12}_{-0.54}$
$B^0 \rightarrow \rho^0\phi \rightarrow (\pi^+\pi^-)(K^+K^-)$	$1.02^{+1.12}_{-0.54}$	$-1.02^{+1.12}_{-0.54}$	0	$1.02^{+1.12}_{-0.54}$	0	$1.02^{+1.12}_{-0.54}$
$B_s^0 \rightarrow \rho^0\phi \rightarrow (\pi^+\pi^-)(K^+K^-)$	$-4.91^{+0.30}_{-0.24}$	$-0.08^{+0.73}_{-0.76}$	$-2.50^{+0.43}_{-0.37}$	$-2.42^{+0.25}_{-0.32}$	$-2.72^{+0.44}_{-0.35}$	$-2.64^{+0.36}_{-0.27}$

$(-20.92^{+6.26}_{-2.80})\%$ of the $B^0 \rightarrow \rho^0\phi \rightarrow (\pi^+\pi^-)(K^+K^-)$ decay simply reflect the final-state strong phases.

As usual, the decay amplitude associated with transverse polarization A_{\parallel} is smaller than that for longitudinal polarization A_0 in the SM within factorization. This indicates that \mathcal{A}_T^2 is power suppressed relative to \mathcal{A}_T^1 . Meanwhile, the smallness of \mathcal{A}_T^2 is also attributed to the suppression from the strong phase difference between the perpendicular and parallel polarization amplitudes, which is supported by the previous PQCD calculations [23]. An observation of \mathcal{A}_T^2 with large values can signify physics beyond the SM. All these PQCD predictions can be tested in the near future.

5 Conclusion

By employing the perturbative QCD factorization approach, we have systematically investigated the four-body decays $B_{(s)} \rightarrow (\pi\pi)(K\bar{K})$ under the quasi-two-body approximation, in which the $\pi\pi$ and $K\bar{K}$ invariant-mass spectrum are dominated by the vector resonances ρ^0 and ϕ , respectively. The scalar resonance $f_0(980)$ is also contributed in the selected $\pi\pi$ and $K\bar{K}$ invariant-mass ranges. The strong dynamics associated with the hadronization of the final state meson pairs is parametrized into the non-perturbative two-meson DAs, which include both resonant and nonresonant contributions and have been established in three-body B meson decays. With the two-meson DAs, the branching ratios, polarization fractions, direct CP asymmetries, and the triple product asymmetries of the four-body decays $B_{(s)} \rightarrow [\rho\phi, \rho f_0, f_0\phi, f_0 f_0] \rightarrow (\pi\pi)(K\bar{K})$ have been examined.

Under the narrow width approximation equation, the two-body $B_{(s)} \rightarrow \rho\phi$ branching ratios have been extracted from the results for the four-body decays $B_{(s)} \rightarrow \rho\phi \rightarrow (\pi\pi)(K\bar{K})$. We also presented the polarization fractions of the related four-body decays. The obtained two-body branch-

ing ratio $\mathcal{B}(B_s^0 \rightarrow \rho^0\phi)$ is consistent well with the previous two-body PQCD prediction and the current experimental data within errors. The calculated large longitudinal polarization fractions $f_0 \sim 90\%$ of the $B_{(s)} \rightarrow \rho\phi$ decay modes also agree well with the theoretical predictions from the previous PQCD, QCDF, SCET and FAT approaches.

We calculated the direct CP asymmetries and TPAs of the four-body $B_{(s)} \rightarrow (\pi\pi)(K\bar{K})$ decays. For the two pure penguin $B^0 \rightarrow \rho^0\phi \rightarrow (\pi^+\pi^-)(K^+K^-)$ and $B^+ \rightarrow \rho^+\phi \rightarrow (\pi^+\pi^0)(K^+K^-)$ decays, both the direct CP asymmetries and “true” TPAs are naturally expected to be zero in the SM due to the vanishing weak phase difference. While for $B_s^0 \rightarrow \rho^0\phi \rightarrow (\pi^+\pi^-)(K^+K^-)$ channel, the magnitude of the $\mathcal{A}_{\text{dir}}^{\text{CP}}$ and $\mathcal{A}_{T\text{-true}}^1$ can exceed 20% and 10% respectively, which are expected to be confronted with the future experiments. The “fake” TPAs requiring no weak phase difference are usually nonzero for all decay channels. The predicted sizable $\mathcal{A}_{T\text{-fake}}^1 = (-20.92^{+6.26}_{-2.80})\%$ of the $B^0 \rightarrow \rho^0\phi \rightarrow (\pi^+\pi^-)(K^+K^-)$ decay simply reflects the importance of the strong final-state interactions.

Acknowledgements Many thanks to H.n. Li for valuable discussions. This work was supported by the National Natural Science Foundation of China under the No. 12075086, No. 12105028. ZR is supported in part by the Natural Science Foundation of Hebei Province under Grant No. A2021209002 and No. A2019209449.

Data Availability Statement This manuscript has no associated data. [Authors’ comment: All data analysed in this manuscript are available from the corresponding author on reasonable request.]

Code Availability Statement This manuscript has no associated code/software. [Authors’ comment: Code/Software sharing not applicable to this article as no code/software was generated or analysed during the current study.]

Open Access This article is licensed under a Creative Commons Attribution 4.0 International License, which permits use, sharing, adaptation, distribution and reproduction in any medium or format, as long as you give appropriate credit to the original author(s) and the source, provide a link to the Creative Commons licence, and indicate if changes

were made. The images or other third party material in this article are included in the article’s Creative Commons licence, unless indicated otherwise in a credit line to the material. If material is not included in the article’s Creative Commons licence and your intended use is not permitted by statutory regulation or exceeds the permitted use, you will need to obtain permission directly from the copyright holder. To view a copy of this licence, visit <http://creativecommons.org/licenses/by/4.0/>. Funded by SCOAP³.

Appendix A: S-wave decay amplitudes

According to Eq. (42), the total decay amplitudes of the S-wave channels can be divided into the $n\bar{n} = \frac{1}{\sqrt{2}}(u\bar{u} + d\bar{d})$ and $s\bar{s}$ components,

- $B_{(s)} \rightarrow [\rho f_0, f_0\phi] \rightarrow (\pi\pi)(K\bar{K})$ decay modes

$$\begin{aligned}
 &A(B^+ \rightarrow \rho^+ f_n \rightarrow (\pi^+\pi^0)(K^+K^-)) \\
 &= \frac{G_F}{2} V_{ub}^* V_{ud} \left[\left(C_2 + \frac{C_1}{3} \right) (F_{ef_n}^{LL} + F_{af_n}^{LL} + F_{ap}^{LL}) \right. \\
 &\quad \left. + C_1 (M_{ef_n}^{LL} + M_{af_n}^{LL} + M_{ap}^{LL}) + C_2 M_{ep}^{LL} \right] \\
 &\quad - \frac{G_F}{2} V_{tb}^* V_{td} \left[\left(C_4 + \frac{C_3}{3} + C_{10} + \frac{C_9}{3} \right) \right. \\
 &\quad \left. (F_{ef_n}^{LL} + F_{af_n}^{LL} + F_{ap}^{LL}) \right. \\
 &\quad \left. + \left(C_6 + \frac{C_5}{3} + C_8 + \frac{C_7}{3} \right) (F_{af_n}^{SP} + F_{ap}^{SP}) \right. \\
 &\quad \left. + \left(2C_6 + \frac{C_8}{2} \right) M_{ep}^{SP} \right. \\
 &\quad \left. + \left(C_6 + \frac{C_5}{3} - \frac{C_8}{2} - \frac{C_7}{6} \right) \right. \\
 &\quad \left. F_{ep}^{SP} + \left(C_5 - \frac{C_7}{2} \right) M_{ep}^{LR} \right. \\
 &\quad \left. + (C_3 + C_9) (M_{ef_n}^{LL} + M_{af_n}^{LL} + M_{ap}^{LL}) \right. \\
 &\quad \left. + (C_5 + C_7) (M_{ef_n}^{LR} + M_{af_n}^{LR} + M_{ap}^{LR}) \right. \\
 &\quad \left. + \left(C_3 + 2C_4 - \frac{C_9}{2} + \frac{C_{10}}{2} \right) M_{ep}^{LL} \right], \tag{A1}
 \end{aligned}$$

$$\begin{aligned}
 &A(B^+ \rightarrow \rho^+ f_s \rightarrow (\pi^+\pi^0)(K^+K^-)) \\
 &= -\frac{G_F}{\sqrt{2}} V_{tb}^* V_{td} \left[\left(C_4 - \frac{C_{10}}{2} \right) M_{ep}^{LL} \right. \\
 &\quad \left. + \left(C_6 - \frac{C_8}{2} \right) M_{ep}^{SP} \right], \tag{A2}
 \end{aligned}$$

$$\begin{aligned}
 &2A(B^0 \rightarrow \rho^0 f_n \rightarrow (\pi^+\pi^-)(K^+K^-)) \\
 &= \frac{G_F}{\sqrt{2}} V_{ub}^* V_{ud} \left[\left(C_1 + \frac{C_2}{3} \right) (F_{ef_n}^{LL} \right. \right. \\
 &\quad \left. \left. + F_{af_n}^{LL} + F_{ap}^{LL}) \right. \right. \\
 &\quad \left. \left. + C_2 (M_{ef_n}^{LL} + M_{af_n}^{LL} + M_{ep}^{LL} + M_{ap}^{LL}) \right] \right]
 \end{aligned}$$

$$\begin{aligned}
 &- \frac{G_F}{\sqrt{2}} V_{tb}^* V_{td} \left[\left(-C_4 - \frac{C_3}{3} + \frac{3C_7}{2} \right. \right. \\
 &\quad \left. \left. + \frac{C_8}{2} + \frac{3C_9}{2} + \frac{C_{10}}{2} + \frac{C_{10}}{2} + \frac{C_9}{6} \right) \right. \\
 &\quad \left. \times (F_{ef_n}^{LL} + F_{af_n}^{LL} + F_{ap}^{LL}) \right. \\
 &\quad \left. + \left(-C_6 - \frac{C_5}{3} + \frac{C_8}{2} + \frac{C_7}{6} \right) (F_{ep}^{SP} \right. \\
 &\quad \left. + F_{af_n}^{SP} + F_{ap}^{SP}) \right. \\
 &\quad \left. - \left(C_3 - \frac{C_9}{2} - \frac{3C_{10}}{2} \right) (M_{ef_n}^{LL} + M_{af_n}^{LL} + M_{ap}^{LL}) \right. \\
 &\quad \left. - \left(2C_6 + \frac{C_8}{2} \right) M_{ep}^{SP} - \left(C_3 + 2C_4 - \frac{C_9}{2} \right. \right. \\
 &\quad \left. \left. + \frac{C_{10}}{2} \right) M_{ep}^{LL} \right. \\
 &\quad \left. + \frac{3C_8}{2} (M_{ef_n}^{SP} + M_{af_n}^{SP} + M_{ap}^{SP}) \right. \\
 &\quad \left. - \left(C_5 - \frac{C_7}{2} \right) (M_{ef_n}^{LR} \right. \\
 &\quad \left. + M_{af_n}^{LR} + M_{ep}^{LR} + M_{ap}^{LR}) \right], \tag{A3}
 \end{aligned}$$

$$\begin{aligned}
 &A(B^0 \rightarrow \rho^0 f_s \rightarrow (\pi^+\pi^-)(K^+K^-)) \\
 &= -\frac{G_F}{2} V_{tb}^* V_{td} \left[\left(-C_4 + \frac{C_{10}}{2} \right) M_{ep}^{LL} \right. \\
 &\quad \left. + \left(-C_6 + \frac{C_8}{2} \right) M_{ep}^{SP} \right], \tag{A4}
 \end{aligned}$$

$$\begin{aligned}
 &2A(B_s^0 \rightarrow \rho^0 f_n \rightarrow (\pi^+\pi^-)(K^+K^-)) \\
 &= \frac{G_F}{\sqrt{2}} V_{ub}^* V_{us} \left[\left(C_1 + \frac{C_2}{3} \right) (F_{af_n}^{LL} + F_{ap}^{LL}) \right. \\
 &\quad \left. + C_2 (M_{af_n}^{LL} + M_{ap}^{LL}) \right] \\
 &\quad - \frac{G_F}{\sqrt{2}} V_{tb}^* V_{ts} \left[\left(\frac{3C_7}{2} \right. \right. \\
 &\quad \left. \left. + \frac{C_8}{2} + \frac{3C_9}{2} + \frac{C_{10}}{2} \right) (F_{af_n}^{LL} + F_{ap}^{LL}) \right. \\
 &\quad \left. + \frac{3C_{10}}{2} (M_{af_n}^{LL} + M_{ap}^{LL}) \right. \\
 &\quad \left. + \frac{3C_8}{2} (M_{af_n}^{SP} + M_{ap}^{SP}) \right], \tag{A5}
 \end{aligned}$$

$$\begin{aligned}
 &A(B_s^0 \rightarrow \rho^0 f_s \rightarrow (\pi^+\pi^-)(K^+K^-)) \\
 &= \frac{G_F}{2} \left\{ V_{ub}^* V_{us} \left[\left(C_1 + \frac{C_2}{3} \right) F_{efs}^{LL} \right. \right. \\
 &\quad \left. \left. + C_2 M_{efs}^{LL} \right] \right. \\
 &\quad \left. - V_{tb}^* V_{ts} \left[\frac{3}{2} \left(C_7 + \frac{C_8}{3} \right) \right. \right. \\
 &\quad \left. \left. + C_9 + \frac{C_{10}}{3} \right) F_{efs}^{LL} \right. \right. \\
 &\quad \left. \left. + \frac{3C_{10}}{2} M_{efs}^{LL} + \frac{3C_8}{2} M_{efs}^{SP} \right] \right\}, \tag{A6}
 \end{aligned}$$

$$\begin{aligned}
 &A(B^0 \rightarrow f_n \phi \rightarrow (\pi^+ \pi^-)(K^+ K^-)) \\
 &= -\frac{G_F}{2} V_{tb}^* V_{td} \\
 &\left[\left(C_3 + \frac{C_4}{3} + C_5 + \frac{C_6}{3} - \frac{C_7}{2} - \frac{C_8}{6} \right. \right. \\
 &\quad \left. \left. - \frac{C_9}{2} - \frac{C_{10}}{6} \right) F_{ef_n}^{LL,h} \right. \\
 &\quad \left. + \left(2C_4 + \frac{C_{10}}{2} \right) M_{ef_n}^{LL} \right. \\
 &\quad \left. + \left(2C_6 + \frac{C_8}{2} \right) M_{ef_n}^{SP} \right], \tag{A7}
 \end{aligned}$$

$$\begin{aligned}
 &A(B^0 \rightarrow f_s \phi \rightarrow (\pi^+ \pi^-)(K^+ K^-)) \\
 &= -\frac{G_F}{\sqrt{2}} V_{tb}^* V_{td} \left[\left(C_3 + \frac{C_4}{3} + C_5 + \frac{C_6}{3} \right. \right. \\
 &\quad \left. \left. - \frac{C_7}{2} - \frac{C_8}{6} - \frac{C_9}{2} - \frac{C_{10}}{6} \right) \right. \\
 &\quad \times (F_{af_s}^{LL,h} + F_{a\phi}^{LL,h}) \\
 &\quad \left. + \left(2C_4 + \frac{C_{10}}{2} \right) (M_{af_s}^{LL} + M_{a\phi}^{LL}) \right. \\
 &\quad \left. + \left(2C_6 + \frac{C_8}{2} \right) (M_{af_s}^{SP} + M_{a\phi}^{SP}) \right], \tag{A8}
 \end{aligned}$$

$$\begin{aligned}
 &A(B_s^0 \rightarrow f_n \phi \rightarrow (\pi^+ \pi^-)(K^+ K^-)) \\
 &= \frac{G_F}{2} V_{ub}^* V_{us} [C_2 M_{e\phi}^{LL}] \\
 &\quad - \frac{G_F}{2} V_{tb}^* V_{ts} \left[\left(2C_4 + \frac{C_{10}}{2} \right) M_{e\phi}^{LL} \right. \\
 &\quad \left. + \left(2C_6 + \frac{C_8}{2} \right) M_{e\phi}^{SP} \right], \tag{A9}
 \end{aligned}$$

$$\begin{aligned}
 &A(B_s^0 \rightarrow f_s \phi \rightarrow (\pi^+ \pi^-)(K^+ K^-)) \\
 &= -\frac{G_F}{\sqrt{2}} V_{tb}^* V_{ts} \left[\left(C_5 - \frac{C_7}{2} \right) \right. \\
 &\quad \left(M_{e\phi}^{LR} + M_{a\phi}^{LR} + M_{ef_s}^{LR} + M_{af_s}^{LR} \right) \\
 &\quad + \frac{4}{3} \left(C_3 + C_4 - \frac{C_9}{2} - \frac{C_{10}}{2} \right) \\
 &\quad \left(F_{ef_s}^{LL} + F_{a\phi}^{LL} + F_{af_s}^{LL} \right) \\
 &\quad + \left(C_6 - \frac{C_8}{2} \right) (M_{ef_s}^{SP} + M_{af_s}^{SP} \\
 &\quad + M_{e\phi}^{SP} + M_{a\phi}^{SP}) \\
 &\quad + \left(C_3 + C_4 - \frac{C_9}{2} - \frac{C_{10}}{2} \right) (M_{e\phi}^{LL} + M_{a\phi}^{LL} \\
 &\quad + M_{ef_s}^{LL} + M_{af_s}^{LL}) \\
 &\quad \left. + \left(C_5 + \frac{C_6}{3} - \frac{C_7}{2} - \frac{C_8}{6} \right) \right. \\
 &\quad \left. (F_{ef_s}^{LR} + F_{a\phi}^{LR} + F_{af_s}^{LR}) \right]
 \end{aligned}$$

$$\begin{aligned}
 &+ \left(C_6 + \frac{C_5}{3} - \frac{C_8}{2} - \frac{C_7}{6} \right) (F_{e\phi}^{SP} \\
 &\quad + F_{a\phi}^{SP} + F_{af_s}^{SP})]. \tag{A10}
 \end{aligned}$$

The decay amplitudes for the physical states are then

$$\begin{aligned}
 &A(B_{(s)} \rightarrow [\rho f_0, f_0 \phi] \rightarrow (\pi \pi)(K \bar{K})) \\
 &= A(B_{(s)} \rightarrow [\rho f_n, f_n \phi] \rightarrow (\pi \pi)(K \bar{K})) \sin \theta \\
 &+ A(B_{(s)} \rightarrow [\rho f_s, f_s \phi] \rightarrow (\pi \pi)(K \bar{K})) \cos \theta. \tag{A11}
 \end{aligned}$$

- $B_{(s)} \rightarrow f_0 f_0 \rightarrow (\pi \pi)(K \bar{K})$ decay modes

$$\begin{aligned}
 &2A(B^0 \rightarrow f_n f_n \rightarrow (\pi^+ \pi^-)(K^+ K^-)) \\
 &= \frac{G_F}{\sqrt{2}} V_{ub}^* V_{ud} \left[\left(C_1 + \frac{C_2}{3} \right) (F_{af_n}^{LL}) \right. \\
 &\quad \left. + C_2 (M_{ef_n}^{LL} + M_{af_n}^{LL}) \right] \\
 &\quad - \frac{G_F}{\sqrt{2}} V_{tb}^* V_{td} \left[\left(2C_3 + \frac{2C_4}{3} + C_4 + \frac{C_3}{3} + 2C_5 \right. \right. \\
 &\quad \left. \left. + \frac{2C_6}{3} + \frac{C_7}{2} + \frac{C_8}{6} \right. \right. \\
 &\quad \left. \left. + \frac{C_9}{2} + \frac{C_{10}}{6} - \frac{C_{10}}{2} - \frac{C_9}{6} \right) F_{af_n}^{LL} \right. \\
 &\quad + \left(C_6 + \frac{C_5}{3} - \frac{C_8}{2} - \frac{C_7}{6} \right) (F_{ef_n}^{SP} + F_{af_n}^{SP}) \\
 &\quad + \left(C_3 + 2C_4 - \frac{C_9}{2} + \frac{C_{10}}{2} \right) (M_{ef_n}^{LL} + M_{af_n}^{LL}) \\
 &\quad + \left(C_5 - \frac{C_7}{2} \right) (M_{ef_n}^{LR} + M_{af_n}^{LR}) \\
 &\quad + \left(2C_6 + \frac{C_8}{2} \right) (M_{ef_n}^{SP} + M_{af_n}^{SP}) \\
 &\quad \left. + [(f_n \rightarrow K^+ K^-) \leftrightarrow (f_n \rightarrow \pi^+ \pi^-)], \tag{A12}
 \end{aligned}$$

$$\begin{aligned}
 &A(B^0 \rightarrow f_n f_s \rightarrow (\pi^+ \pi^-)(K^+ K^-)) \\
 &= -\frac{G_F}{2} V_{tb}^* V_{td} \left[\left(C_4 - \frac{C_{10}}{2} \right) M_{ef_n}^{LL} \right. \\
 &\quad \left. + \left(C_6 - \frac{C_8}{2} \right) M_{ef_n}^{SP} \right], \tag{A13}
 \end{aligned}$$

$$\begin{aligned}
 &A(B^0 \rightarrow f_s f_s \rightarrow (\pi^+ \pi^-)(K^+ K^-)) \\
 &= -\frac{G_F}{\sqrt{2}} V_{tb}^* V_{td} \left[\left(C_3 + \frac{C_4}{3} + C_5 + \frac{C_6}{3} \right. \right. \\
 &\quad \left. \left. - \frac{C_7}{2} - \frac{C_8}{6} - \frac{C_9}{2} - \frac{C_{10}}{6} \right) F_{af_s}^{LL} \right. \\
 &\quad + \left(C_4 - \frac{C_{10}}{2} \right) M_{af_s}^{LL} \\
 &\quad + \left(C_6 - \frac{C_8}{2} \right) M_{af_s}^{SP} \\
 &\quad \left. + [(f_s \rightarrow K^+ K^-) \leftrightarrow (f_s \rightarrow \pi^+ \pi^-)], \tag{A14}
 \end{aligned}$$

$$\begin{aligned}
 &2A(B_s^0 \rightarrow f_n f_n \rightarrow (\pi^+ \pi^-)(K^+ K^-)) \\
 &= \frac{G_F}{\sqrt{2}} V_{ub}^* V_{us} \left[\left(C_1 + \frac{C_2}{3} \right) F_{af_n}^{LL} + C_2 M_{af_n}^{LL} \right] \\
 &\quad - \frac{G_F}{\sqrt{2}} V_{tb}^* V_{ts} \left[\left(2C_3 + \frac{2C_4}{3} + 2C_5 + \frac{2C_6}{3} + \frac{C_7}{2} \right. \right. \\
 &\quad \left. \left. + \frac{C_8}{6} + \frac{C_9}{2} + \frac{C_{10}}{6} \right) F_{af_n}^{LL} \right. \\
 &\quad \left. + \left(2C_4 + \frac{C_{10}}{2} \right) M_{af_n}^{LL} \right. \\
 &\quad \left. + \left(2C_6 + \frac{C_8}{2} \right) M_{af_n}^{SP} \right] \\
 &+ [(f_n \rightarrow K^+ K^-) \leftrightarrow (f_n \rightarrow \pi^+ \pi^-)], \tag{A15}
 \end{aligned}$$

$$\begin{aligned}
 &A(B_s^0 \rightarrow f_n f_s \rightarrow (\pi^+ \pi^-)(K^+ K^-)) \\
 &= \frac{G_F}{2} V_{ub}^* V_{us} \left[C_2 M_{ef_s}^{LL} \right] \\
 &\quad - \frac{G_F}{2} V_{tb}^* V_{ts} \left[\left(2C_4 + \frac{C_{10}}{2} \right) M_{ef_s}^{LL} \right. \\
 &\quad \left. + \left(2C_6 + \frac{C_8}{2} \right) M_{ef_s}^{SP} \right], \tag{A16}
 \end{aligned}$$

$$\begin{aligned}
 &A(B_s^0 \rightarrow f_s f_s \rightarrow (\pi^+ \pi^-)(K^+ K^-)) \\
 &= -\frac{G_F}{\sqrt{2}} V_{tb}^* V_{ts} \left[\left(C_3 + \frac{C_4}{3} + C_4 + \frac{C_3}{3} - \frac{C_9}{2} \right. \right. \\
 &\quad \left. \left. - \frac{C_{10}}{6} - \frac{C_{10}}{2} - \frac{C_9}{6} \right) F_{af_s}^{LL} \right. \\
 &\quad \left. + \left(C_6 + \frac{C_5}{3} - \frac{C_8}{2} - \frac{C_7}{6} \right) \right. \\
 &\quad \left. \left(F_{ef_s}^{SP} + F_{af_s}^{SP} \right) \right. \\
 &\quad \left. + \left(C_3 + C_4 - \frac{C_9}{2} - \frac{C_{10}}{2} \right) \left(M_{ef_s}^{LL} + M_{af_s}^{LL} \right) \right. \\
 &\quad \left. + \left(C_5 - \frac{C_7}{2} \right) \left(M_{ef_s}^{LR} + M_{af_s}^{LR} \right) \right. \\
 &\quad \left. + \left(C_6 - \frac{C_8}{2} \right) \left(M_{ef_s}^{SP} + M_{af_s}^{SP} \right) \right] \\
 &+ [(f_s \rightarrow K^+ K^-) \leftrightarrow (f_s \rightarrow \pi^+ \pi^-)]. \tag{A17}
 \end{aligned}$$

The decay amplitudes for the physical states are then

$$\begin{aligned}
 &A(B_{(s)} \rightarrow f_0 f_0 \rightarrow (\pi\pi)(K\bar{K})) \\
 &= A(B_{(s)} \rightarrow f_n f_n \rightarrow (\pi\pi)(K\bar{K}))(\sin \theta)^2 \\
 &\quad + A(B_{(s)} \rightarrow f_n f_s \rightarrow (\pi\pi)(K\bar{K})) \sin 2\theta \\
 &\quad + A(B_{(s)} \rightarrow f_s f_s \rightarrow (\pi\pi)(K\bar{K}))(\cos \theta)^2. \tag{A18}
 \end{aligned}$$

Appendix B: Two-meson distribution amplitudes

The two-meson DA usually depends on the parton momentum fraction x , the meson momentum fraction ζ , which

describes the relative motion between the two mesons in the pair, and the meson-pair invariant mass squared ω^2 . One can decompose a two-meson DA in eigenfunctions of the QCD evolution equation (the Gegenbauer polynomials $C_n^{3/2}(2x - 1)$) and in partial waves of the produced meson pair (the Legendre polynomials $P_l(2\zeta - 1)$). The expansion of a two-meson DA in terms of the two sets of orthogonal polynomials then reads [61,131]

$$\begin{aligned}
 \Phi(x, \zeta, \omega^2) &= \frac{6}{2\sqrt{2N_c}} x(1-x) \sum_{n=0}^{\infty} \sum_{l=0}^{n+1} B_{nl}(\omega^2) \\
 &C_n^{3/2}(2x - 1) P_l(2\zeta - 1), \tag{B1}
 \end{aligned}$$

where $B_{nl}(\omega^2)$ are the ω^2 -dependent coefficients, $N_c = 3$ is the number of colors, and $l = 0, 1, 2, \dots$ denote the S -wave, P -wave, D -wave, ... components, respectively.

The S -wave two-meson DAs can be written as [132] ($h_1 h_2 = \pi\pi, K\bar{K}$),

$$\begin{aligned}
 \Phi_{(h_1 h_2)_S}(z, \zeta, \omega) &= \frac{1}{\sqrt{2N_c}} [\not{P} \phi_{(h_1 h_2)_S}^0(z, \zeta, \omega^2) \\
 &\quad + \omega \phi_{(h_1 h_2)_S}^S(z, \zeta, \omega^2) \\
 &\quad + \omega (\not{P} - 1) \phi_{(h_1 h_2)_S}^T(z, \zeta, \omega^2)], \tag{B2}
 \end{aligned}$$

in which N_c is the number of colors, and the asymptotic forms of the various twists DAs are parametrized as [57–60]

$$\phi_{(h_1 h_2)_S}^0(x, \zeta, \omega^2) = \frac{9F_S(\omega^2)}{\sqrt{2N_c}} a_{h_1 h_2} x(1-x)(1-2x), \tag{B3}$$

$$\phi_{(h_1 h_2)_S}^S(x, \zeta, \omega^2) = \frac{F_S(\omega^2)}{2\sqrt{2N_c}}, \tag{B4}$$

$$\phi_{(h_1 h_2)_S}^T(x, \zeta, \omega^2) = \frac{F_S(\omega^2)}{2\sqrt{2N_c}} (1 - 2x), \tag{B5}$$

with the time-like scalar form factor $F_S(\omega^2)$. Because the Legendre polynomial $P_0(2\zeta - 1)$ is unity for the S wave meson pairs, the dependence of the ζ does not show up in above functions. The Gegenbauer moments $a_{h_1 h_2}$ in Eq. (B3) are adopted the same values as those determined in Refs. [133,134]: $a_{\pi\pi} = 0.20 \pm 0.20$ [133], $a_{KK} = 0.80 \pm 0.16$ [134].

The elastic rescattering effects in the final-state meson pair can usually be absorbed into the time-like form factor $F(\omega^2)$ according to the Watson theorem [135]. For the scalar resonance $f_0(980)$, its pole mass is very close to the $K\bar{K}$ threshold, which can have strong influence on the resonance shape. In the present work, we follow Refs. [136,137] to employ the widely used Flatté model suggested by Bugg [138],

$$F_S(\omega^2) = \frac{m_{f_0(980)}^2}{m_{f_0(980)}^2 - \omega^2 - im_{f_0(980)}(g_{\pi\pi}\rho_{\pi\pi} + g_{KK}\rho_{KK}F_{KK}^2)}, \tag{B6}$$

with the two phase space factors $\rho_{\pi\pi}$ and ρ_{KK} [64, 136, 139]

$$\begin{aligned} \rho_{\pi\pi} &= \frac{2}{3}\sqrt{1 - \frac{4m_{\pi^\pm}^2}{\omega^2}} + \frac{1}{3}\sqrt{1 - \frac{4m_{\pi^0}^2}{\omega^2}}, \\ \rho_{KK} &= \frac{1}{2}\sqrt{1 - \frac{4m_{K^\pm}^2}{\omega^2}} + \frac{1}{2}\sqrt{1 - \frac{4m_{K^0}^2}{\omega^2}}. \end{aligned} \tag{B7}$$

The $g_{\pi\pi} = 0.167$ GeV and $g_{KK} = 3.47g_{\pi\pi}$ [136, 137] are coupling constants, describing the f_0 decay into the final states $\pi^+\pi^-$ and K^+K^- , respectively. The exponential factor $F_{KK} = e^{-\alpha q_k^2}$ is introduced above the $K\bar{K}$ threshold to reduce the ρ_{KK} factor as invariant mass increases, where q_k is the momentum of the kaon in the $K\bar{K}$ rest frame and $\alpha = 2.0 \pm 0.25\text{GeV}^{-2}$ [136, 138].

The corresponding P -wave two-meson DAs related to both longitudinal and transverse polarizations are decomposed, up to the twist 3, into [140]:

$$\begin{aligned} \Phi_{(h_1h_2)_P}^L(x, \zeta, \omega) &= \frac{1}{\sqrt{2N_c}} \left[\omega \not{\epsilon}_P \phi_{(h_1h_2)_P}^0(x, \zeta, \omega^2) \right. \\ &\quad + \omega \phi_{(h_1h_2)_P}^s(x, \zeta, \omega^2) \\ &\quad \left. + \frac{\not{p}_1 \not{p}_2 - \not{p}_2 \not{p}_1}{\omega(2\zeta - 1)} \phi_{(h_1h_2)_P}^t(x, \zeta, \omega^2) \right], \end{aligned} \tag{B8}$$

$$\begin{aligned} \Phi_{(h_1h_2)_P}^T(x, \zeta, \omega) &= \frac{1}{\sqrt{2N_c}} \left[\gamma_5 \not{\epsilon}_T \not{p} \phi_{(h_1h_2)_P}^T(x, \zeta, \omega^2) \right. \\ &\quad + \omega \gamma_5 \not{\epsilon}_T \phi_{(h_1h_2)_P}^a(x, \zeta, \omega^2) \\ &\quad \left. + i\omega \frac{\epsilon^{\mu\nu\rho\sigma} \gamma_\mu \epsilon_{T\nu} p_\rho n_{-\sigma}}{p \cdot n_-} \phi_{(h_1h_2)_P}^v(x, \zeta, \omega^2) \right]. \end{aligned} \tag{B9}$$

The various twist DAs $\phi_{(h_1h_2)_P}^i$ in the above equations can be expanded in terms of the Gegenbauer polynomials:

$$\begin{aligned} \phi_{\pi\pi}^0(x_1, \zeta_1, \omega_1^2) &= \frac{3F_{\pi\pi}^\parallel(\omega_1^2)}{\sqrt{2N_c}} x_1(1-x_1) \\ &\quad \times \left[1 + a_{2\rho}^0 \frac{3}{2}(5(1-2x_1)^2 - 1) \right] (2\zeta_1 - 1), \end{aligned} \tag{B10}$$

$$\begin{aligned} \phi_{\pi\pi}^s(x_1, \zeta_1, \omega_1^2) &= \frac{3F_{\pi\pi}^\perp(\omega_1^2)}{2\sqrt{2N_c}} (1-2x_1) \\ &\quad \times \left[1 + a_{2\rho}^s (10x_1^2 - 10x_1 + 1) \right] (2\zeta_1 - 1), \end{aligned} \tag{B11}$$

$$\begin{aligned} \phi_{\pi\pi}^t(x_1, \zeta_1, \omega_1^2) &= \frac{3F_{\pi\pi}^\perp(\omega_1^2)}{2\sqrt{2N_c}} (1-2x_1)^2 \\ &\quad \times \left[1 + a_{2\rho}^t \frac{3}{2}(5(1-2x_1)^2 - 1) \right] (2\zeta_1 - 1), \end{aligned} \tag{B12}$$

$$\phi_{\pi\pi}^T(x_1, \zeta_1, \omega_1^2) = \frac{3F_{\pi\pi}^\perp(\omega_1^2)}{\sqrt{2N_c}} x_1(1-x_1)$$

$$\times \left[1 + a_{2\rho}^T \frac{3}{2}(5(1-2x_1)^2 - 1) \right] \sqrt{\zeta_1(1-\zeta_1) + \alpha_1}, \tag{B13}$$

$$\begin{aligned} \phi_{\pi\pi}^a(x_1, \zeta_1, \omega_1^2) &= \frac{3F_{\pi\pi}^\parallel(\omega_1^2)}{4\sqrt{2N_c}} (1-2x_1) \\ &\quad \times \left[1 + a_{2\rho}^a (10x_1^2 - 10x_1 + 1) \right] \sqrt{\zeta_1(1-\zeta_1) + \alpha_1}, \end{aligned} \tag{B14}$$

$$\begin{aligned} \phi_{\pi\pi}^v(x_1, \zeta_1, \omega_1^2) &= \frac{3F_{\pi\pi}^\parallel(\omega_1^2)}{8\sqrt{2N_c}} \left\{ [1 + (1-2x_1)^2] \right. \\ &\quad \left. + a_{2\rho}^v [3(2x_1 - 1)^2 - 1] \right\} \sqrt{\zeta_1(1-\zeta_1) + \alpha_1}, \end{aligned} \tag{B15}$$

$$\begin{aligned} \phi_{KK}^0(x_2, \zeta_2, \omega_2^2) &= \frac{3F_{KK}^\parallel(\omega_2^2)}{\sqrt{2N_c}} x_2(1-x_2) \\ &\quad \times \left[1 + a_{2\phi}^0 \frac{3}{2}(5(1-2x_2)^2 - 1) \right] (2\zeta_2 - 1), \end{aligned} \tag{B16}$$

$$\phi_{KK}^s(x_2, \zeta_2, \omega_2^2) = \frac{3F_{KK}^\perp(\omega_2^2)}{2\sqrt{2N_c}} (1-2x_2)(2\zeta_2 - 1), \tag{B17}$$

$$\phi_{KK}^t(x_2, \zeta_2, \omega_2^2) = \frac{3F_{KK}^\perp(\omega_2^2)}{2\sqrt{2N_c}} (1-2x_2)^2(2\zeta_2 - 1), \tag{B18}$$

$$\begin{aligned} \phi_{KK}^T(x_2, \zeta_2, \omega_2^2) &= \frac{3F_{KK}^\perp(\omega_2^2)}{\sqrt{2N_c}} x_2(1-x_2) \\ &\quad \times \left[1 + a_{2\phi}^T \frac{3}{2}(5(1-2x_2)^2 - 1) \right] \sqrt{\zeta_2(1-\zeta_2) + \alpha_2}, \end{aligned} \tag{B19}$$

$$\begin{aligned} \phi_{KK}^a(x_2, \zeta_2, \omega_2^2) &= \frac{3F_{KK}^\parallel(\omega_2^2)}{4\sqrt{2N_c}(1-2x_2)} \sqrt{\zeta_2(1-\zeta_2) + \alpha_2}, \end{aligned} \tag{B20}$$

$$\begin{aligned} \phi_{KK}^v(x_2, \zeta_2, \omega_2^2) &= \frac{3F_{KK}^\parallel(\omega_2^2)}{8\sqrt{2N_c}} [1 + (1-2x_2)^2] \sqrt{\zeta_2(1-\zeta_2) + \alpha_2}, \end{aligned} \tag{B21}$$

with the P -wave form factors $F_{\pi\pi}^{\parallel(\perp)}(\omega^2)$ and $F_{KK}^{\parallel(\perp)}(\omega^2)$. The values of the Gegenbauer moments associated with longitudinal and transverse polarization components are adopted the same as those in Refs. [72, 73, 86, 140]:

$$\begin{aligned} a_{2\phi}^0 &= 0.40 \pm 0.06, & a_{2\phi}^T &= 1.48 \pm 0.07, \\ a_{2\rho}^0 &= 0.39 \pm 0.11, & a_{2\rho}^s &= -0.34 \pm 0.26, \\ a_{2\rho}^t &= -0.13 \pm 0.04, \\ a_{2\rho}^T &= 0.50 \pm 0.50, & a_{2\rho}^a &= 0.40 \pm 0.40, \\ a_{2\rho}^v &= -0.50 \pm 0.50. \end{aligned} \tag{B22}$$

Because the amounts of the current experimental data are not yet enough for fixing the Gegenbauer moments in the twist-

3 DAs $\phi_{KK}^{s,t}$ and $\phi_{KK}^{v,a}$, they have been set to the asymptotic forms in our work.

In the experimental analysis of the multi-body hadronic B meson decays, the contribution from the wide ρ resonant is usually parameterized as the Gounaris-Sakurai (GS) model [66] based on the BW function [65]. By taking the $\rho - \omega$ interference and the excited states into account, the form factor $F_{\pi\pi}^{\parallel}(\omega^2)$ can be written in the form of [141]

$$F_{\pi\pi}^{\parallel}(\omega^2) = \left[\text{GS}_{\rho}(s, m_{\rho}, \Gamma_{\rho}) \frac{1 + c_{\omega}\text{BW}_{\omega}(s, m_{\omega}, \Gamma_{\omega})}{1 + c_{\omega}} + \sum_i c_i \text{GS}_i(s, m_i, \Gamma_i) \right] \left[1 + \sum_i c_i \right]^{-1} \quad (\text{B23})$$

where $s = \omega^2$ is the two-pion invariant mass squared, $i = (\rho'(1450), \rho''(1700), \rho'''(2254))$, $\Gamma_{\rho,\omega,i}$ is the decay width for the relevant resonance, $m_{\rho,\omega,i}$ are the masses of the corresponding mesons, respectively. The explicit expressions of the function $\text{GS}_{\rho}(s, m_{\rho}, \Gamma_{\rho})$ can be written as [65]

$$\text{GS}_{\rho}(s, m_{\rho}, \Gamma_{\rho}) = \frac{m_{\rho}^2 [1 + d(m_{\rho})\Gamma_{\rho}/m_{\rho}]}{m_{\rho}^2 - s + f(s, m_{\rho}, \Gamma_{\rho}) - im_{\rho}\Gamma(s, m_{\rho}, \Gamma_{\rho})}, \quad (\text{B24})$$

with the factors

$$\begin{aligned} d(m) &= \frac{3}{\pi} \frac{m_{\pi}^2}{k^2(m^2)} \ln \left(\frac{m + 2k(m^2)}{2m_{\pi}} \right) \\ &\quad + \frac{m}{2\pi k(m^2)} - \frac{m_{\pi}^2 m}{\pi k^3(m^2)}, \\ f(s, m, \Gamma) &= \frac{\Gamma m^2}{k^3(m^2)} \left[k^2(s)[h(s) - h(m^2)] \right. \\ &\quad \left. + (m^2 - s)k^2(m^2)h'(m^2) \right], \\ \Gamma(s, m_{\rho}, \Gamma_{\rho}) &= \Gamma_{\rho} \frac{s}{m_{\rho}^2} \left(\frac{\beta_{\pi}(s)}{\beta_{\pi}(m_{\rho}^2)} \right)^3. \end{aligned} \quad (\text{B25})$$

The functions $k(s)$, $h(s)$ and $\beta_{\pi}(s)$ can be expressed as

$$\begin{aligned} k(s) &= \frac{1}{2} \sqrt{s} \beta_{\pi}(s), \quad h(s) = \frac{2}{\pi} \frac{k(s)}{\sqrt{s}} \ln \left(\frac{\sqrt{s} + 2k(s)}{2m_{\pi}} \right), \\ \beta_{\pi}(s) &= \sqrt{1 - 4m_{\pi}^2/s}. \end{aligned} \quad (\text{B26})$$

For the vector form factor of the $K\bar{K}$ system, the dominant resonance is $\phi(1020)$ in the concerned mass window. We then employ the relativistic BW line shape to parameterize the $F_{KK}^{\parallel}(\omega^2)$ [142],

$$F_{KK}^{\parallel}(\omega^2) = \frac{m_{\phi}^2}{m_{\phi}^2 - \omega^2 - im_{\phi}\Gamma_{\phi}(\omega^2)}, \quad (\text{B27})$$

with the mass-dependent width $\Gamma_{\phi}(\omega^2)$

$$\Gamma_{\phi}(\omega^2) = \Gamma_{\phi} \left(\frac{m_{\phi}}{\omega} \right) \left(\frac{k(\omega)}{k(m_{\phi})} \right)^{(2L_R+1)}. \quad (\text{B28})$$

The $m_{\phi} = 1.0195$ GeV [87] and $\Gamma_{\phi} = 4.25$ MeV [87] represent the mass and natural width of the ϕ meson, respectively. The orbital angular momentum L_R in the two-meson system is set to $L_R = 1$ for a P -wave state. The $k(\omega)$ is the momentum vector of the resonance decay product measured in the resonance rest frame, while $k(m_{\phi})$ is the value of $k(\omega)$ when $\omega = m_{\phi}$. Due to the limited studies on the form factor $F^{\perp}(\omega^2)$, we usually assume the approximation $F^{\perp}(\omega^2)/F^{\parallel}(\omega^2) \approx f_V^T/f_V$ in our calculation, with $f_V^{(T)}$ being the vector (tensor) decay constants of the intermediate vector resonance.

References

1. A. Datta, M. Duraisamy, D. London, Searching for new physics with B -decay fake triple products. *Phys. Lett. B* **701**, 357 (2011)
2. M. Beneke, J. Rohrer, D.S. Yang, Branching fractions, polarisation and asymmetries of $B \rightarrow VV$ decays. *Nucl. Phys. B* **774**, 64 (2007)
3. H.Y. Cheng, C.K. Chua, K.C. Yang, Charmless B decays to a scalar meson and a vector meson. *Phys. Rev. D* **77**, 014034 (2008)
4. H.Y. Cheng, C.K. Chua, Revisiting charmless hadronic $B_{u,d}$ decays in QCD factorization. *Phys. Rev. D* **80**, 114008 (2009)
5. H.Y. Cheng, C.K. Chua, QCD factorization for charmless hadronic B_s decays revisited. *Phys. Rev. D* **80**, 114026 (2009)
6. Y. Li, E.L. Wang, Branching fractions and CP asymmetries of $B \rightarrow K_0^*(1430)\rho$ and $B \rightarrow K_0^*(1430)\phi$ decays in the family nonuniversal Z' model. [arXiv:1206.4106](https://arxiv.org/abs/1206.4106)
7. H.Y. Cheng, C.K. Chua, K.C. Yang, Z.Q. Zhang, Revisiting charmless hadronic B decays to scalar mesons. *Phys. Rev. D* **87**, 114001 (2013)
8. C.D. Lü, Y.L. Shen, C. Wang, Y.M. Wang, Enhanced next-to-leading-order corrections to weak annihilation B -meson decays. *Nucl. Phys. B* **990**, 116175 (2023)
9. Hn. Li, Resolution to the $B \rightarrow \phi K^*$ polarization puzzle. *Phys. Lett. B* **622**, 63 (2005)
10. J. Zhu, Y.L. Shen, C.D. Lü, Polarization, CP asymmetry, and branching ratios in $B \rightarrow K^*K^*$ with the perturbative QCD approach. *Phys. Rev. D* **72**, 054015 (2005)
11. J. Zhu, Y.L. Shen, C.D. Lü, $B_s \rightarrow \rho(\omega)K^*$ with perturbative QCD approach. *J. Phys. G* **32**, 101 (2006)
12. H.W. Huang, C.D. Lü, T. Morii, Y.L. Shen, G.L. Song, J. Zhu, Study of $B \rightarrow K^*\rho, K^*\omega$ decays with polarization in the perturbative QCD approach. *Phys. Rev. D* **73**, 014011 (2006)
13. W. Wang, Y.L. Shen, Y. Li, C.D. Lü, Study of scalar mesons $f_0(980)$ and $f_0(1500)$ from $B \rightarrow f_0(980)K$ and $B \rightarrow f_0(1500)K$ Decays. *Phys. Rev. D* **74**, 114010 (2006)
14. Y. Li, C.D. Lü, Branching ratio and polarization of $B \rightarrow \rho(\omega)\rho(\omega)$ decays in perturbative QCD approach. *Phys. Rev. D* **73**, 014024 (2006)
15. A. Ali, G. Kramer, Y. Li, C.D. Lü, Y.L. Shen, W. Wang, Y.M. Wang, Charmless nonleptonic B_s decays to PP, PV , and VV final states in the perturbative QCD approach. *Phys. Rev. D* **76**, 074018 (2007)
16. C.S. Kim, Y. Li, W. Wang, Study of decay modes $B \rightarrow K_0^*(1430)\phi$. *Phys. Rev. D* **81**, 074014 (2010)

17. Z.Q. Zhang, J.D. Zhang, Study of scalar meson $f_0(980)$ from $B \rightarrow f_0(980)K^*$ Decays. *Eur. Phys. J. C* **67**, 163 (2010)
18. Z.Q. Zhang, Study of scalar meson $f_0(980)$ and $K_0^*(1430)$ from $B \rightarrow f_0(980)\rho(\omega, \phi)$ and $B \rightarrow K_0^*(1430)\rho(\omega)$ decays. *Phys. Rev. D* **82**, 034036 (2010)
19. X. Liu, Z.J. Xiao, Z.T. Zou, Branching ratios and CP violations of $B \rightarrow K_0^*(1430)K^*$ decays in the perturbative QCD approach. *Phys. Rev. D* **88**, 094003 (2013)
20. Z.W. Liu, Z.T. Zou, Y. Li, X. Liu, J. Wang, Charmless $B_s \rightarrow VS$ decays in PQCD approach. *Eur. Phys. J. C* **82**, 59 (2022)
21. Z.R. Liang, X.Q. Yu, Perturbative QCD predictions for the decay $B_s^0 \rightarrow SS(a_0(980), f_0(980), f_0(500))$. *Phys. Rev. D* **102**, 116007 (2020)
22. H.D. Niu, G.D. Li, J.L. Ren, X. Liu, Perturbative QCD analysis of neutral B -meson decays into $\sigma\sigma, \sigma f_0$ and $f_0 f_0$. *Eur. Phys. J. C* **82**, 177 (2022)
23. Z.T. Zou, A. Ali, C.D. Lü, X. Liu, Y. Li, Improved estimates of the $B_{(s)} \rightarrow VV$ decays in perturbative QCD approach. *Phys. Rev. D* **91**, 054033 (2015)
24. D.C. Yan, X. Liu, Z.J. Xiao, Anatomy of $B_s \rightarrow VV$ decays and effects of next-to-leading order contributions in the perturbative QCD factorization approach. *Nucl. Phys. B* **935**, 17 (2018)
25. C.W. Bauer, D. Pirjol, I.Z. Rothstein, I.W. Stewart, $B \rightarrow M_1 M_2$: factorization, charming penguins, strong phases, and polarization. *Phys. Rev. D* **70**, 054015 (2004)
26. C.W. Bauer, I.Z. Rothstein, I.W. Stewart, SCET analysis of $B \rightarrow K\pi, B \rightarrow K\bar{K}$, and $B \rightarrow \pi\pi$ decays. *Phys. Rev. D* **74**, 034010 (2006)
27. M. Beneke, Y. Kiyo, D.S. Yang, Loop corrections to subleading heavy quark currents in SCET. *Nucl. Phys. B* **692**, 232 (2004)
28. M. Beneke, G. Buchalla, M. Neubert, C.T. Sachrajda, Comment on “ $B \rightarrow M_1 M_2$: factorization, charming penguins, strong phases, and polarization”. *Phys. Rev. D* **72**, 098501 (2005)
29. C.W. Bauer, D. Pirjol, I.Z. Rothstein, I.W. Stewart, On differences between SCET and QCDF for $B \rightarrow \pi\pi$ decays. *Phys. Rev. D* **72**, 098502 (2005)
30. C. Wang, S.H. Zhou, Y. Li, C.D. Lü, Global analysis of charmless B decays into two vector mesons in soft-collinear effective theory. *Phys. Rev. D* **96**, 073004 (2017)
31. C. Wang, Q.A. Zhang, Y. Li, C.D. Lü, Charmless $B_{(s)} \rightarrow VV$ decays in factorization-assisted topological-amplitude approach. *Eur. Phys. J. C* **77**, 333 (2017)
32. R. Itoh et al. [Belle Collaboration], Studies of CP violation in $B \rightarrow J/\psi K^*$ decays. *Phys. Rev. Lett.* **95**, 091601 (2005)
33. B. Aubert et al. [BABAR Collaboration], Measurement of decay amplitudes of $B \rightarrow J/\psi K^*, \psi(2S)K^*$, and $\chi_{c1}K^*$ with an angular analysis. *Phys. Rev. D* **76**, 031102 (2007)
34. T. Aaltonen et al. [CDF Collaboration], Measurement of polarization and search for CP violation in $B_s^0 \rightarrow \phi\phi$ decays. *Phys. Rev. Lett.* **107**, 261802 (2011)
35. R. Aaij et al. [LHCb Collaboration], Measurement of the polarization amplitudes and triple product asymmetries in the $B_s^0 \rightarrow \phi\phi$ decay. *Phys. Lett. B* **713**, 369 (2012)
36. R. Aaij et al. [LHCb Collaboration], First measurement of the CP -violating phase in $B_s^0 \rightarrow \phi\phi$ decays. *Phys. Rev. Lett.* **110**, 241802 (2013)
37. R. Aaij et al. [LHCb Collaboration], Measurement of CP violation in $B_s^0 \rightarrow \phi\phi$ decays. *Phys. Rev. D* **90**, 052011 (2014)
38. R. Aaij et al. [LHCb Collaboration], Measurement of CP asymmetries and polarisation fractions in $B_s^0 \rightarrow K^{*0}\bar{K}^{*0}$ decays. *J. High Energy Phys.* **07**, 166 (2015)
39. R. Aaij et al. [LHCb Collaboration], Study of the $B^0 \rightarrow \rho(770)^0 K^*(892)^0$ decay with an amplitude analysis of $B^0 \rightarrow (\pi^+\pi^-)(K^+\pi^-)$ decays. *J. High Energy Phys.* **05**, 026 (2019)
40. R. Aaij et al. [LHCb Collaboration], Measurement of polarization amplitudes and CP asymmetries in $B^0 \rightarrow \phi K^*(892)^0$. *J. High Energy Phys.* **05**, 069 (2014)
41. R. Aaij et al. [LHCb Collaboration], Measurement of CP violation in the $B_s^0 \rightarrow \phi\phi$ decay and search for the $B^0 \rightarrow \phi\phi$ decay. *J. High Energy Phys.* **12**, 155 (2019)
42. G. Valencia, Angular correlations in the decay $B \rightarrow VV$ and CP violation. *Phys. Rev. D* **39**, 3339 (1989)
43. B. Kayser, Kinematically nontrivial CP violation in beauty decay. *Nucl. Phys. B Proc. Suppl.* **13**, 487 (1990)
44. A. Datta, D. London, Triple-product correlations in $B \rightarrow V_1 V_2$ decays and new physics. *Int. J. Mod. Phys. A* **19**, 2505 (2004)
45. M. Gronau, J.L. Rosner, Triple-product asymmetries in $K, D_{(s)}$, and $B_{(s)}$ decays. *Phys. Rev. D* **84**, 096013 (2011)
46. A. Datta, M. Duraisamy, D. London, New physics in $\bar{b} \rightarrow \bar{s}$ transitions and the $B_{d,s}^0 \rightarrow V_1 V_2$ angular analysis. *Phys. Rev. D* **86**, 076011 (2012)
47. B. Bhattacharya, A. Datta, M. Duraisamy, D. London, Searching for new physics with $\bar{b} \rightarrow \bar{s} B_s^0 \rightarrow V_1 V_2$ penguin decays. *Phys. Rev. D* **88**, 016007 (2013)
48. G. Durieux, Y. Grossman, Probing CP violation systematically in differential distributions. *Phys. Rev. D* **92**, 076013 (2015)
49. S.K. Patra, A. Kundu, CPT violation and triple-product correlations in B decays. *Phys. Rev. D* **87**, 116005 (2013)
50. J.P. Wang, Q. Qin, F.S. Yu, CP violation induced by T-odd correlations and its baryonic application. [arXiv:2211.07332](https://arxiv.org/abs/2211.07332)
51. R. Aaij et al. [LHCb Collaboration], Observation of the decay $B_s^0 \rightarrow \phi\pi^+\pi^-$ and evidence for $B^0 \rightarrow \phi\pi^+\pi^-$. *Phys. Rev. D* **95**, 012006 (2017)
52. A. Ali, J.G. Körner, G. Kramer, J. Willrodt, Nonleptonic weak decays of bottom mesons. *Z. Phys. C* **1**, 269 (1979)
53. M. Suzuki, Final-state interactions and s -quark helicity conservation in $B \rightarrow J/\psi K^*$. *Phys. Rev. D* **64**, 117503 (2001)
54. K.F. Chen et al. [Belle Collaboration], Measurement of branching fractions and polarization in $B \rightarrow \phi K^{(*)}$ decays. *Phys. Rev. Lett.* **91**, 201801 (2003)
55. B. Aubert et al. [BABAR Collaboration], Time-Dependent and Time-Integrated Angular Analysis of $B \rightarrow \phi K_S \pi^0$ and $\phi K^\pm \pi^\mp$. *Phys. Rev. D* **78**, 092008 (2008)
56. J.P. Lees et al. [BABAR Collaboration], B^0 meson decays to $\rho^0 K^{*0}, f_0 K^{*0}$, and $\rho^- K^{*+}$, including higher K^* resonances. *Phys. Rev. D* **85**, 072005 (2012)
57. D. Müller, D. Robaschik, B. Geyer, F.M. Dittes, J. Hořejši, Wave functions, evolution equations and evolution kernels from light ray operators of QCD. *Fortschr. Physik.* **42**, 101 (1994)
58. M. Diehl, T. Gousset, B. Pire, O. Teryaev, Probing partonic structure in $\gamma^*\gamma \rightarrow \pi\pi$ near threshold. *Phys. Rev. Lett.* **81**, 1782 (1998)
59. M. Diehl, T. Gousset, B. Pire, Exclusive production of pion pairs in $\gamma^*\gamma$ collisions at large Q^2 . *Phys. Rev. D* **62**, 073014 (2000)
60. Ph. Hägler, B. Pire, L. Szymanowski, O.V. Teryaev, Pomeron-odderon interference effects in electroproduction of two pions. *Eur. Phys. J. C* **26**, 261 (2002)
61. M.V. Polyakov, Hard exclusive electroproduction of two pions and their resonances. *Nucl. Phys. B* **555**, 231 (1999)
62. A.G. Grozin, On wave functions of mesonic pairs and mesonic resonances. *Sov. J. Nucl. Phys.* **38**, 289 (1983)
63. A.G. Grozin, One- and two-particle wave functions of multi-hadron systems. *Theor. Math. Phys.* **69**, 1109 (1986)
64. S.M. Flatté, On the nature of 0^+ mesons. *Phys. Lett. B* **63**, 228 (1976)
65. G. Breit, E. Wigner, Capture of slow neutrons. *Phys. Rev.* **49**, 519 (1936)
66. G. Gounaris, J.J. Sakurai, Final-width corrections to the vector-meson-dominance prediction for $\rho \rightarrow e^+e^-$. *Phys. Rev. Lett.* **21**, 244 (1968)

67. J.J. Qi, Z.Y. Wang, J. Xu, X.H. Guo, Studying the localized CP violation and the branching fraction of the $\bar{B}^0 \rightarrow K^- \pi^+ \pi^+ \pi^-$ decay. *Chin. Phys. C* **44**, 103104 (2020)
68. J.J. Qi, Z.Y. Wang, X.H. Guo, Phenomenological studies on the $\bar{B}^0 \rightarrow [K^- \pi^+]_{S/P} [\pi^+ \pi^-]_{V/S} \rightarrow K^- \pi^+ \pi^+ \pi^-$ decay. *Chin. Phys. C* **45**, 053104 (2021)
69. Z. Rui, Y. Li, H.N. Li, Four-body decays $B_{(s)} \rightarrow (K\pi)_{S/P} (K\pi)_{S/P}$ in the perturbative QCD approach. *J. High Energy Phys.* **05**, 082 (2021)
70. Y. Li, D.C. Yan, Z. Rui, Z.J. Xiao, Study of $B_{(s)} \rightarrow (\pi\pi)(K\pi)$ decays in the perturbative QCD approach. *Eur. Phys. J. C* **81**, 806 (2021)
71. C.Q. Zhang, J.M. Li, M.K. Jia, Y. Li, Z. Rui, CP -violating observables in four-body $B \rightarrow \phi(\rightarrow K\bar{K})K^*(\rightarrow K\pi)$ decays. *Phys. Rev. D* **105**, 053002 (2022)
72. D.C. Yan, Z. Rui, Z.J. Xiao, Y. Li, Study of $B_{(s)}^0 \rightarrow \phi\phi \rightarrow (K^+K^-)(K^+K^-)$ decays in the perturbative QCD approach. *Phys. Rev. D* **105**, 093001 (2022)
73. D.C. Yan, Z. Rui, Y. Yan, Y. Li, Study of four-body decays $B_{(s)} \rightarrow (\pi\pi)(\pi\pi)$ in the perturbative QCD approach. *Eur. Phys. J. C* **83**, 974 (2023)
74. H.Q. Liang, X.Q. Yu, Study of the four-body decays $B_s^0 \rightarrow N_1 N_2 \rightarrow \pi\pi\pi\pi$ in the perturbative QCD approach. *Phys. Rev. D* **105**, 096018 (2022)
75. G. Buchalla, A.J. Buras, M.E. Lautenbacher, Weak decays beyond leading logarithms. *Rev. Mod. Phys.* **68**, 1125 (1996)
76. Hn. Li, QCD aspects of exclusive B meson decays. *Prog. Part. Nucl. Phys.* **51**, 85 (2003)
77. T. Kurimoto, Hn. Li, A.I. Sanda, Leading power contributions to $B \rightarrow \pi, \rho$ transition form factors. *Phys. Rev. D* **65**, 014007 (2002)
78. W. Wang, Y.M. Wang, J. Xu, S. Zhao, B -meson light-cone distribution amplitude from the Euclidean quantity. *Phys. Rev. D* **102**, 011502(R) (2020)
79. Hn. Li, H.S. Liao, B meson wave function in k_T factorization. *Phys. Rev. D* **70**, 074030 (2004)
80. Hn. Li, Y.L. Shen, Y.M. Wang, Resummation of rapidity logarithms in B meson wave functions. *J. High Energy Phys.* **02**, 008 (2013)
81. Hn. Li, Y.M. Wang, Non-dipolar Wilson links for transverse-momentum-dependent wave functions. *J. High Energy Phys.* **06**, 013 (2015)
82. Hn. Li, Y.L. Shen, Y.M. Wang, Next-to-leading-order corrections to $B \rightarrow \pi$ form factors in k_T factorization. *Phys. Rev. D* **85**, 074004 (2012)
83. Q. Qin, Y.L. Shen, C. Wang, Y.M. Wang, Deciphering the long-distance penguin contribution to $\bar{B}_{d,s} \rightarrow \gamma\gamma$ decays. *Phys. Rev. Lett.* **131**, 091902 (2023)
84. S. Cheng, A. Khodjamirian, J. Virto, $B \rightarrow \pi\pi$ form factors from light-cone sum rules with B -meson distribution amplitudes. *J. High Energy Phys.* **05**, 157 (2017)
85. C.D. Lü, Y.L. Shen, C. Wang, Y.M. Wang, Shedding new light on weak annihilation B -meson decays. *Nucl. Phys. B* **990**, 116175 (2023)
86. Y. Li, D.C. Yan, J. Hua, Z. Rui, H.N. Li, Global determination of two-meson distribution amplitudes from three-body B decays in the perturbative QCD approach. *Phys. Rev. D* **104**, 096014 (2021)
87. R.L. Workman et al. [Particle Data Group], Review of particle physics. *Prog. Theor. Exp. Phys.* **2022**, 083C01 (2022)
88. C.Q. Geng, Y.K. Hsiao, Rare $B^- \rightarrow \Lambda \bar{p} \nu \bar{\nu}$ decay. *Phys. Rev. D* **85**, 094019 (2012)
89. Y.K. Hsiao, C.Q. Geng, Four-body baryonic decays of $B \rightarrow p \bar{p} \pi^+ \pi^- (\pi^+ K^-)$ and $\Lambda \bar{\Lambda} \pi^+ \pi^- (\pi^+ K^-)$. *Phys. Lett. B* **770**, 348 (2017)
90. J. Hua, Hn. Li, C.D. Lü, W. Wang, Z.P. Xing, Global analysis of hadronic two-body B decays in the perturbative QCD approach. *Phys. Rev. D* **104**, 016025 (2021)
91. Y.Y. Keum, Hn. Li, A.I. Sanda, Fat penguins and imaginary penguins in perturbative QCD. *Phys. Lett. B* **504**, 6 (2001)
92. C.D. Lü, K. Ukai, M.Z. Yang, Branching ratio and CP violation of $B \rightarrow \pi\pi$ decays in perturbative QCD approach. *Phys. Rev. D* **63**, 074009 (2001)
93. H.Y. Cheng, C.K. Chua, K.C. Yang, Charmless hadronic B decays involving scalar mesons: Implications to the nature of light scalar mesons. *Phys. Rev. D* **73**, 014017 (2006)
94. H.Y. Cheng, Hadronic D decays involving scalar mesons. *Phys. Rev. D* **67**, 034024 (2003)
95. A.V. Anisovich, V.V. Anisovich, V.N. Markov, N.A. Nikonov, Radiative decays and quark content of $f_0(980)$ and $\phi(1020)$. *Phys. At. Nucl.* **65**, 497 (2002)
96. A. Gokalp, Y. Sarac, O. Yilmaz, An Analysis of $f_0 - \sigma$ mixing in light cone QCD sum rules. *Phys. Lett. B* **609**, 291 (2005)
97. L. Yang, Z.T. Zou, Y. Li, X. Liu, C.H. Li, Quasi-two-body $B_{(s)} \rightarrow V\pi\pi$ decays with resonance $f_0(980)$ in the PQCD approach. *Phys. Rev. D* **103**, 113005 (2021)
98. P. Colangelo, F. De Fazio, W. Wang, $B_s \rightarrow f_0(980)$ form factors and B_s decays into $f_0(980)$. *Phys. Rev. D* **81**, 074001 (2010)
99. P. Colangelo, F. De Fazio, W. Wang, Nonleptonic B_s to charmonium decays: Analysis in pursuit of determining the weak phase β_s . *Phys. Rev. D* **83**, 094027 (2011)
100. S. Cheng, J.M. Shen, $\bar{B}_s \rightarrow f_0(980)$ form factors and the width effect from light-cone sum rules. *Eur. Phys. J. C* **80**, 554 (2020)
101. B. Aubert et al. [BABAR Collaboration], Dalitz plot analysis of the decay $B^\pm \rightarrow K^\pm K^\pm K^\mp$. *Phys. Rev. D* **74**, 032003 (2006)
102. M. Ablikim et al. [BES Collaboration], Evidence for $f_0(980)f_0(980)$ production in χ_{c0} decays. *Phys. Rev. D* **70**, 092002 (2004)
103. M. Ablikim et al. [BES Collaboration], Partial wave analysis of $\chi_{c0} \rightarrow \pi^+ \pi^- K^+ K^-$. *Phys. Rev. D* **72**, 092002 (2005)
104. R. Aaij et al. [LHCb Collaboration], Dalitz plot analysis of $B^0 \rightarrow \bar{D}^0 \pi^+ \pi^-$ decays. *Phys. Rev. D* **92**, 032002 (2015)
105. H.Y. Cheng, C.W. Chiang, C.K. Chua, Finite-width effects in three-body B decays. *Phys. Rev. D* **103**, 036017 (2021)
106. H.Y. Cheng, C.W. Chiang, C.K. Chua, Width effects in resonant three-body decays: B decay as an example. *Phys. Lett. B* **813**, 136058 (2021)
107. Z.T. Zou, L. Yang, Y. Li, X. Liu, Study of quasi-two-body $B_{(s)} \rightarrow \phi(f_0(980)/f_2(1270) \rightarrow) \pi\pi$ decays in perturbative QCD approach. *Eur. Phys. J. C* **81**, 91 (2021)
108. Hn. Li, S. Mishima, Polarizations in $B \rightarrow VV$ decays. *Phys. Rev. D* **71**, 054025 (2005)
109. H.Y. Cheng, K.C. Yang, Branching ratios and polarization in $B \rightarrow VV, VA, AA$ decays. *Phys. Rev. D* **78**, 094001 (2008). [Erratum: *Phys. Rev. D* **79**, 039903 (2009)]
110. Y. Grossman, Beyond the standard model with B and K physics. *Int. J. Mod. Phys. A* **19**, 907 (2004)
111. P.K. Das, K.C. Yang, Data for polarization in charmless $B \rightarrow \phi K^*$: a signal for new physics? *Phys. Rev. D* **71**, 094002 (2005)
112. C.H. Chen, C.Q. Geng, Scalar interactions to the polarizations of $B \rightarrow \phi K^*$. *Phys. Rev. D* **71**, 115004 (2005)
113. Y.D. Yang, R.M. Wang, G.R. Lu, Polarizations in decays $B_{u,d} \rightarrow VV$ and possible implications for R-parity violating SUSY. *Phys. Rev. D* **72**, 015009 (2005)
114. A.L. Kagan, Polarization in $B \rightarrow VV$ decays. *Phys. Lett. B* **601**, 151 (2004)
115. M. Beneke, J. Rohrer, D. Yang, Enhanced electroweak penguin amplitude in $B \rightarrow VV$ decays. *Phys. Rev. Lett.* **96**, 141801 (2006)
116. A. Datta, A.V. Gritsan, D. London, M. Nagashima, A. Szybkman, Testing explanations of the $B \rightarrow \phi K^*$ polarization puzzle. *Phys. Rev. D* **76**, 034015 (2007)

117. P. Colangelo, F. De Fazio, T.N. Pham, The riddle of polarization in $B \rightarrow VV$ transitions. *Phys. Lett. B* **597**, 291 (2004)
118. M. Ladisa, V. Laporta, G. Nardulli, P. Santorelli, Final state interactions for $B \rightarrow VV$ charmless decays. *Phys. Rev. D* **70**, 114025 (2004)
119. H.Y. Cheng, C.K. Chua, A. Soni, Final state interactions in hadronic B decays. *Phys. Rev. D* **71**, 014030 (2005)
120. E. Alvarez, L.N. Epele, D. Gomez Dumm, A. Szykman, Right handed currents and FSI phases in $B^0 \rightarrow \phi K^{*0}$. *Phys. Rev. D* **70**, 115014 (2004)
121. K.C. Yang, Annihilation in factorization-suppressed B decays involving a $1^1 P_1$ meson and search for new physics signals. *Phys. Rev. D* **72**, 034009 (2005). [Erratum: *Phys. Rev. D* **72**, 059901 (2005)]
122. S. Baek, A. Datta, P. Hamel, O.F. Hernandez, D. London, Polarization states in $B \rightarrow \rho K^*$ and new physics. *Phys. Rev. D* **72**, 094008 (2005)
123. C.S. Huang, P. Ko, X.H. Wu, Y.D. Yang, MSSM anatomy of the polarization puzzle in $B \rightarrow \phi K^*$ decays. *Phys. Rev. D* **73**, 034026 (2006)
124. C.H. Chen, H. Hatanaka, Nonuniversal Z' couplings in B decays. *Phys. Rev. D* **73**, 075003 (2006)
125. A. Faessler, T. Gutsche, J.C. Helo, S. Kovalenko, V.E. Lyubovitskij, On the possible resolution of the B-meson decay polarization anomaly in R-parity violating SUSY. *Phys. Rev. D* **75**, 074029 (2007)
126. C.H. Chen, C.Q. Geng, Y.K. Hsiao, Z.T. Wei, Productions of $K_0^*(1430)$ and K_1 in B decays. *Phys. Rev. D* **72**, 054011 (2005)
127. C.H. Chen, C.Q. Geng, Expectations on $B \rightarrow (K_0^*(1430), K_2^*(1430))\phi$ decays. *Phys. Rev. D* **75**, 054010 (2007)
128. H.Y. Cheng, K.C. Yang, Charmless hadronic B decays into a tensor meson. *Phys. Rev. D* **83**, 034001 (2011)
129. C. Bobeth, M. Gorbahn, S. Vickers, Weak annihilation and new physics in charmless $B \rightarrow MM$ decays. *Eur. Phys. J. C* **75**, 340 (2015)
130. A.L. Kagan, Polarization in $B \rightarrow VV$ decays. *Phys. Lett. B* **601**, 151 (2004)
131. J. Chai, S. Cheng, A.J. Ma, Probing isovector scalar mesons in the charmless three-body B decays. *Phys. Rev. D* **105**, 033003 (2022)
132. W.F. Wang, Hn. Li, W. Wang, C.D. Lü, S-wave resonance contributions to the $B_{(s)}^0 \rightarrow J/\psi \pi^+ \pi^-$ and $B_s \rightarrow \pi^+ \pi^- \mu^+ \mu^-$ decays. *Phys. Rev. D* **91**, 094024 (2015)
133. Y. Li, A.J. Ma, W.F. Wang, Z.J. Xiao, The S-wave resonance contributions to the three-body decays $B_{(s)}^0 \rightarrow \eta_c f_0(X) \rightarrow \eta_c \pi^+ \pi^-$ in perturbative QCD approach. *Eur. Phys. J. C* **76**, 675 (2016)
134. Z. Rui, Y. Li, H.N. Li, Studies of the resonance components in the B_s decays into charmonia plus kaon pair. *Eur. Phys. J. C* **79**, 792 (2019)
135. K.M. Watson, The effect of final state interactions on reaction cross sections. *Phys. Rev.* **88**, 1163 (1952)
136. R. Aaij et al. [LHCb Collaboration], Measurement of resonant and CP components in $\bar{B}_s^0 \rightarrow J/\psi \pi^+ \pi^-$ decays. *Phys. Rev. D* **89**, 092006 (2014)
137. R. Aaij et al. [LHCb Collaboration], Measurement of the resonant and CP components in $\bar{B}^0 \rightarrow J/\psi \pi^+ \pi^-$ decays. *Phys. Rev. D* **90**, 012003 (2014)
138. D.V. Bugg, Reanalysis of data on $a_0(1450)$ and $a_0(980)$. *Phys. Rev. D* **78**, 074023 (2008)
139. R. Aaij et al. [LHCb Collaboration], Analysis of the resonant components in $\bar{B}^0 \rightarrow J/\psi \pi^+ \pi^-$. *Phys. Rev. D* **87**, 052001 (2013)
140. Z. Rui, Y. Li, Hn. Li, P-wave contributions to $B \rightarrow \psi \pi \pi$ decays in the perturbative QCD approach. *Phys. Rev. D* **98**, 113003 (2018)
141. J.P. Lees et al. [BABAR Collaboration], Precise measurement of the $e^+ e^- \rightarrow \pi^+ \pi^- (\gamma)$ cross section with the initial-state radiation method at BABAR. *Phys. Rev. D* **86**, 032013 (2012)
142. R. Aaij et al. [LHCb Collaboration], Evidence for an $\eta_c(1S)\pi^-$ resonance in $B^0 \rightarrow \eta_c(1S)K^+ \pi^-$ decays. *Eur. Phys. J. C* **78**, 1019 (2018)